João Francisco Carreira Domingues

Investigação e teste de comunicações rádio 5G V2X para suporte à condução autónoma

Research and test of 5G V2X radio communications to support the autonomous driving

Universidade de Aveiro
2021

Departamento de Eletrónica,
Telecomunicações e Informática

João Francisco Carreira Domingues

Investigação e teste de comunicações rádio 5G V2X para suporte à condução autónoma

Research and test of 5G V2X radio communications to support the autonomous driving

Dissertação apresentada à Universidade de Aveiro para cumprimento dos requisitos necessários à obtenção do grau de Mestre em Engenharia Eletrónica e Telecomunicações, realizada sob a orientação científica do Professor Doutor Adão Silva (orientador), Professor Associado do Departamento de Eletrónica, Telecomunicações e Informática da Universidade de Aveiro e do Doutor Roberto Magueta (coorientador), investigador da Allbesmart LDA.

Primeiramente dedico á minha família principalmente pai, mãe, irmã e avós, pelo apoio que me deram ao longo destes últimos anos, visto que pelo contrário não teria sido possível chegar aqui.

Dedico esta dissertação a todos os meus colegas que se tornaram meus amigos, ao longo destes anos, permitindo que fosse possível chegar onde cheguei.

Por fim, agradeço a todos os professores que me acompanharam ao longo destes anos, à Universidade de Aveiro e ao Departamento de Eletrónica Telecomunicações e Informática pelo profissionalismo e empenho na formação de todos.

O júri / The jury

presidente / presidente

Professor Doutor Pedro Miguel Ribeiro Lavrador
Professor Auxiliar do Departamento de Eletrónica, Telecomunicações e Informática da Universidade de Aveiro(orientador)

vogais / examiners committee

Professor Doutor Rui Miguel Henriques Dias Morgado Dinis
Professor Associado com Agregação da Faculdade de Ciências e Tecnologia da Universidade Nova de Lisboa (arguente)

Professor Doutor Adão Paulo Soares da Silva
Professor Auxiliar do Departamento de Eletrónica, Telecomunicações e Informática da Universidade de Aveiro(orientador)

agradecimentos / acknowledgements

I would like to thank to my supervisor Professor Adão Silva and co-supervisors Paulo Marques and Doctor Roberto Magueta, for their continuous support, help, exceptional supervision, mentoring, and review of my thesis document with their expert opinions.

Also, would like to thank to the Instituto de Telecomunicações, IT and to the company Allbesmart, that provided all the hardware, like servers, to conclude my studies and this dissertation.

For last but not less important, would like to thank to the University and to my Department, Department of Electronics, telecommunications and informatic, that provided all the material and learning conditions to graduate during the course of Electronics and Telecommunication Engineer.

palavras-chave 5G-NR, sidelink, V2X, camada física, PSCCH, 3GPP, sistemas em tempo-real

resumo

A geração atual, quinta geração (5G) ainda está a ser sujeita a análise e investigação. O 5G trouxe grandes mudanças na rede móvel, como na velocidade de transferência de dados, na cobertura de rede, entre outros. O 5G permite latência ultrabaixa e confiabilidade muito alta que vem suportar novas aplicações, nomeadamente na área das comunicações veiculares. Inicialmente, apenas alguns serviços básicos como o tráfego eficiente e seguro foram introduzidos usando a comunicação *device to device*(D2D). As interfaces PC5 e Uu foram também introduzidas para sistemas de assistência de direção mais aprimorados e avançados, como o *platooning*, em que os carros afetados poderiam conduzir em conjunto ao usar a comunicação entre eles e alguns sensores, usando a tecnologia Long Term Evolution LTE. A este ponto, D2D está envolvida com a tecnologia veículo para tudo (V2X). Atualmente, o 5G New Radio (NR) V2X fornece-nos um upgrade em termos de camada física, numerologia e forma de onda. Um dos principais problemas nestes sistemas é o processamento em tempo real, o que deveria ser bastante eficiente para que responda dentro do tempo necessário. Algum deste processamento está relacionado ao estudo do *Physical Sidelink Control Channel* (PSCCH).

Portanto, o objetivo principal desta dissertação é projetar um algoritmo de procura eficiente PSCCH eficiente para as comunicações 5G NR V2X sidelink. Primeiro, começamos por perceber o algoritmo de descodificação convencional PSCCH, onde concluímos que é bastante ineficiente para pesquisar o PSCCH, visto que, todo o processamento devia de ser realizado diversas vezes antes de o descodificar com sucesso. No algoritmo proposto, primeiro foram calculadas todas as correlações entre o sinal recebido e o Demodulation Reference Signal (DMRS), enquanto o restante processamento convencional para descodificar o PSCCH apenas é realizado sobre os subcanais com maior correlação, o que leva a uma redução de complexidade mais forte. O algoritmo implementado é avaliado e comparado com o algoritmo convencional cego. Os resultados mostraram uma melhoria na atuação significativa in termos de tempo de execução.

keywords 5G-NR, sidelink, V2X, PSCCH, 3GPP, real-time systems

abstract

The current fifth generation (5G) is still being object of analyses and investigation. The 5G brought major changes in the mobile networking, like the speed of data transfer, network coverage, between others. The 5G allows ultra-low latency and very high reliability, which comes to support new applications, namely in the area of vehicular communications. Initially, only some basic services like the traffic efficiency and safety, using the device-to-device (D2D) communication were introduced. The PC5 and Uu interfaces were also introduced, for enhanced and advanced driving assistance system, like the platooning, in which the effected cars could drive together by using the communication between them and some extended sensors, using the Long Term Evolution (LTE) technology. At this point, the D2D evolved to the vehicle-to-everything (V2X) technology. Currently, the 5G New Radio (NR) V2X give us an upgrade in terms of physical layer, numerology, and waveform. One of the main problems in these systems is the real-time processing, which should be quite efficient in order to respond within the necessary time. Some of this processing is related to searching the Physical Sidelink Control Channel (PSCCH).

Therefore, the main goal of this dissertation is to design an effective PSCCH searching algorithm for 5G NR V2X sidelink communications. First, we started by understanding the PSCCH conventional blinded decoding algorithm, where we realized that this algorithm is quite inefficient to searching the PSCCH, since all the processing should be done several times before successful decoding it. In the proposed algorithm, we firstly compute all the correlations between the received signal and the Demodulation Reference Signal (DMRS), while the remaining conventional processing to decode the PSCCH is only performed over the subchannels with higher correlation, which leads to a strong complexity reduction. The implemented algorithm is evaluated and compared with the conventional blind algorithm. The results have shown a significant performance improvement in terms of runtime.

Contents

Glossary

1G	First Generation
2G	Second Generation
3G	Third Generation
3GPP	3rd Generation Partnership Project
4G	Fourth Generation
5G	fifth Generation
AM	Acknowledged Mode
BLER	Block Error Ratio
BWP	Bandwidth Part
CAM	Cooperative awareness message
CDMA	Code Division Multiple Access
C-ITS	Cooperative Intelligent Transport Systems
CP	Cyclic prefix
CP-OFDM	Cyclic Prefix Orthogonal Frequency Division Multiplexing
CRS	Cell Specified Signal
C-V2X	Cellular Vehicle-to-Everything
D2D	Device to Device
DENM	Decentralized environmental notification message
DL	Downlink
DMRS	Demodulation Reference Signal
DoF	Degrees of Freedom
ECP	Extended Cyclic Prefix
eMBB	Enhanced Mobile Broadband
eNB	Evolved Node B
eV2X	Enhancement Vehicle-to-Everything
FDMA	Frequency Division Multiple Access
FEC	Forward error correction
FR1	Frequency range 1
FR2	Frequency range 2
FRIV	Frequency resource indicator value
gNB	5G Node B
GSM	Global System for Mobile
HSDPA	High Speed Downlink Packet Access
HSUPA	High Speed Uplink Packet Access
ICI	Inter Carrier Interference
IMT-2020	International Mobile Telecommunications-2020
IoT	Industrial Internet of Things
IoV	Internet of Vehicles
ISI	Inter Symbol Interference
ITS	Intelligent Transport Systems
LDPC	Low density parity check
LTE	Long Term Evolution

MAC	Medium Access Control
mMIMO	Massive MIMO
MCS	Modulation and Coding Scheme
MIB	Master Information Block
MIMO	Multiple Input Multiple Output
MMS	Multimedia Messaging Service
MMSE	Minimum mean-squared error
mMTC	Massive Machine Type Communications
mmWave	Millimetre Wave
NCP	Normal Cyclic Prefix
NR	New Radio
OFDM	Orthogonal Frequency Division Multiplexing
OTP	Open Transport Protocol
OWA	Open Wireless Architecture
PDCDP	Packet Data Convergence Protocol
PDU	Protocol Data Units
PHY	Physical Layer
PSBCH	Physical Sidelink Broadcast Channel
PSCCH	Physical Sidelink Control Channel
PSFCH	Physical sidelink feedback channel
PSSCH	Physical sidelink shared channel
QAM	Quadrature amplitude modulation
QPSK	Quadrature phase shift keying
RB	Resource block
RE	Resource element
RF	Radio Frequency
RLC	Radio Link Control
RRC	Radio Resource Control
RSRP	Reference signals received power
RSU	Road-side unit
SAP	Service Access Point
SBA	Service-Based Architecture
SCI	Sidelink Control Information
SCS	Subcarrier spacing
SDAP	Service Data Adaption Protocol
SIB	System block information
SL	Sidelink
SMS	Short Message Service
SNR	Signal-to-noise-ratio
SPS	Semi-Persistent Scheduling
SPSS	Sidelink Primary Synchronization Signal
S-PSS	Sidelink Primary Synchronization Signals
SSSS	Sidelink Secondary Synchronization Signal
TB	Transport Block

TBCC	Tail-Biting Convolutional Code
TBS	Transport Block Size
TDMA	Time Division Multiple Access
TM	Transparent Mode
TRIV	Time resource indicator value
TS	Technical specification
UE	User Equipment
UL	Uplink
UM	Unacknowledged Mode
UMTS	Universal Mobile Telecommunications System
URLLC	Ultra-Reliable and Low Latency Communications
V2G	Vehicle-to-Grid
V2I	Vehicle-to-Infrastructure
V2N	Vehicle-to-Network
V2P	Vehicle-to-Pedestrian
V2V	Vehicle-to-Vehicle
V2X	Vehicular-to-Everything
WiMAX	Worldwide Interoperability for Microwave Access
SSB	Synchronization Signal Block
CRC	cyclic redundancy check
SL-MIB	Sidelink Master Information Block
SL-BCH	Sidelink Broadcast Channel

List of figures

List of tables

Chapter 1 – Introduction

Wireless communication has evolved since the classic 1G in 1980's years, to the recent 5G which started to emerge in the 2018's years. This evolution brought major changes in the technology that we use, the speed of data transfer, the capacity and finally the network coverage. With the beginning of standardization, each cellular mobile radio generation was projected to provide specific telecommunications services for the mobile terminal. This chapter contains an overview fort the evolution from the 1G to the 5G, it also describes the motivation, the objectives, and contributions of proposed work.

1.1 – Evolution of cellular communications systems: From the 1st to the 5th

The origins of mobile communications followed quickly behind the invention of radio in the late 1800's, where this radio concept was first developed to be used in communication between the different ships at the sea, to make these ships safer there [1]. In the early 1970's, the evolution of the mobile wireless industry was initiated, and soon this technology started to expand. Subsequently in the past few decades, several generations of mobile wireless technologies have been revealed, namely 1G to 5G.

The quick advances and development in the field of mobile and telecommunication sector, proves that this evolution of network generation must be one of the greatest technologies ever seen. It all started with the 1G mobile system which was used to transmit only the analogue signals followed by the second generation (2G) mobile technologies which transmitted digital signals. The third generation (3G) technology brings higher data transmission speed compared to 2G. Fourth generation (4G) of mobile technology was known as LTE, which included many services such as entertainment, multimedia, mobile applications and many more. Finally, the fifth generation (5G) mobile technology was based on OWA (Open Wireless Architecture) and Open Transport Protocol (OTP) [2] and compared with the four previous network generation, brings for example, less latency, higher data traffic and peak rates, higher bandwidth, and connection density.

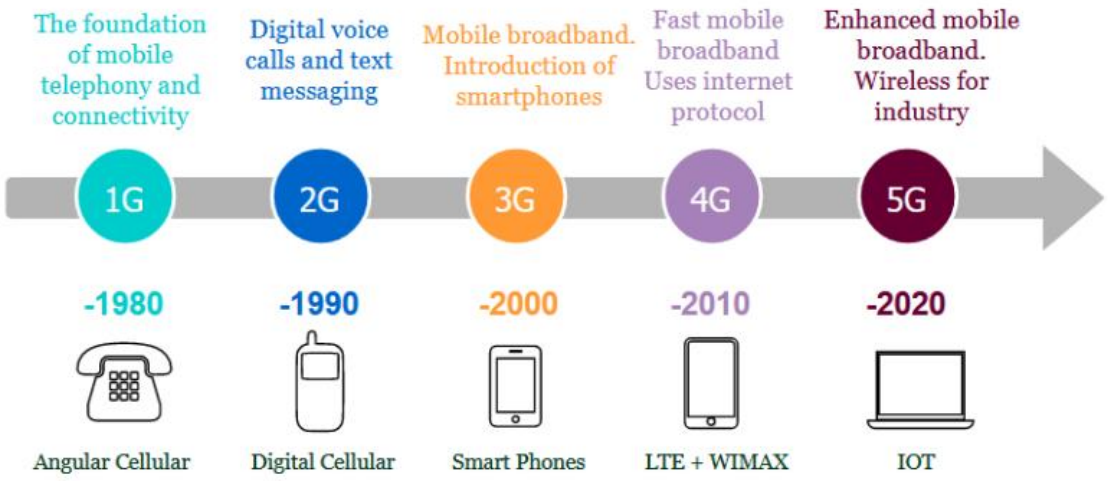

Figure 1. The evolution of mobile technologies [3].

The **Figure 1** presents a schematic of the evolution of mobile technologies, that starts with the First Generation,1G, in 1980 to the Fifth Generation, 5G, that appears nowadays in 2020:

First Generation

The 1G of mobile networks were totally conditional upon analogue radio systems, based on circuit switched technology. It was only used to transmit analogue signals which was created exclusively for voice service, had a lot of limited coverage, capacity, was very expensive, and the users could not send or receive the voice call was modulated at higher frequencies around 150 MHz, and using the technique Frequency Division Multiple Access, FDMA, and transmitted between radio towers. To make it work, cell towers were built around the country, and the signal coverage could be obtained from greater distances. Although, 1G network was unreliable and that started to be a little poor for the users, so the emergency of evolution from the mobile telecommunications, was mandatory, because of the exponential growth of the user subscription. As so it, was necessary to improve some features, such as the analogue system and the limited coverage and capacity, with an advanced mobile network technology, the Second Generation, which instead of using the traditional analogue radio signals, started using the digital signals [2].

Second Generation

The leap between the First and the 2G brought some new features to the mobile communications systems. Firstly, the replacement from the analogue domain to the digital domain, the 2G also provides a new service over the voice service, transmitted with digital signal, with frequency bandwidth in order of 20 to 200 KHz and speed up to 64kbp, this new service provides the possibility to exchange data services between users, such as Short Message Service (SMS) and Multimedia Messaging Service (MMS). For these services to occur, the Global System for Mobile

(GSM) technology was developed the GSM technology, global system for mobile communication or GSM uses digital modulation to improve the voice quality but the networks offered the limited data services.2G carrier continued to improve the transmission quality and coverage, the 2G technologies can be based on Time Division Multiple Access, TDMA, Code Division Multiple Access, CDMA, standards depending on the type of multiplexing used. Also, 2G makes use of the CODEC, compression decompression algorithm, to compress and multiplex Digital voice data. For these capabilities the 2G mobile technology also improves coverage, capacity and affordability, with regard for the mobile technologies, but with the growth of the demands by the users on devices like the mobile phones, the mobile network had to evolve into the third generation (3G)[4][5].

Third Generation

The 3G was revolutionary in the way we observe the mobile technologies, because 3G bring the multimedia cell phone or as we call nowadays, smart phone, where entertainment services, multimedia, and mobile applications, between many others, were added as a feature, like the Fast Communication Internet, Mobile TV, Video Conferencing, Video Calls, MMS, 3D gaming, between other features. To account for these new capabilities was developed HSDPA (High Speed Downlink Packet Access) is a mobile telephony protocol also called 3.5G, it provides higher speed than 3G, 8.1Mbit/sec data transmission, and the HSUPA (High Speed Uplink Packet Access) is a complementary of HSDPA. These new features that were revealed in mobile communications systems, besides revolutionizing the whole idea of mobile networks, forced the appearance of even more sophisticated terminals with greedy applications, demanding higher data rates, increase in system capacity, coverage, and mobility [2][4].

Fourth Generation

The 4G of cellular wireless standards more known as the LTE which is like the 3G in all the features that 3G has, like the MMS and the Digital television in High definition. But this new evolution it is faster and smoother than the introduced the IP-based networks for voice, video, broadcasting media and internet access, offering speed rates on the order of 100Mbps, at high speeds, five times faster than the 3G network. Under 4G, users could experience better latency, in other words less buffering, higher voice quality, easy access to instant messaging services and social media, high quality streaming and faster downloads.

Pre-4G technologies such as mobile Worldwide Interoperability for Microwave Access (WiMAX) and first-release 3G LTE have been available on the market since 2006 and 2009 respectively, basically it is the extension in the 3G technology with more bandwidth and services offers in the 3G. While first LTE mobile phone appeared in 2010, with many network characteristics

such as enabling auto reconfiguration mode. The purpose of 4G systems was not only to support the next generation of mobile service, but also to support the fixed wireless networks [6][4].

Fifth Generation

1G, 2G, 3G, and 4G were mainly about connecting the people, because of the provided services allowing user to connect with each other, accessing to the internet between other services. 5G takes the traditional mobile broadband to the extreme in terms of data rates, capacity, and availability. These capabilities of providing services in a very high rate up to 20 Gbps with a higher capacity, that it is up to 1000 times higher, enabling new services such as Industrial Internet of Things (IoT). Connectivity and critical communications, meaning the connection from the applications, appliances, sensors, objects, and devices with the internet and this requires transmitting, collecting, analysing, and processing data in an efficient network. The features of 5G, include as well driving safety, bringing the vehicular communications, that will allow the driving of autonomous vehicles and can drastically reduce the deaths and accidents that occurs nowadays, between other examples of 5G applications. The expectation of this one it is affecting all the sectors of society by improving the efficiency, the productivity, safety and spreading the concept of the cloud in wireless networks, as well increasing the use of artificial intelligence. To achieve all these new ways to think, the 5G design and deployment must be different from the other evolutions of network generation, in other words, there is a need to completely achieve these targets by using for example, the Massive MIMO (mMIMO) beamforming and millimetre Wave (mmWave) bands to achievement the frequency spectrum and therefore exploiting high data rates and capacity.

In the following **Figure 2**, there is a schematic of the use of 5G and its features, exemplifying that, the 5G has the goal to providing high security and reliability with low latency by order of milliseconds, achieving ultra-fast mobile Internet, also achieving a high broadcasting data, in Gbps, to support almost 6500 connections.

Also there is identified in the *Figure 2* the vehicular communications, which one it is going to bring the possibility of the vehicles communicate between them, open the possibility of the vehicles drive autonomously with the help of other vehicles, also the vehicle communicates with other infrastructures as well the infrastructure of highway, and also an vehicle has the possibility to communicate with pedestrians that are walking on the street. All this possible but real features could help prevent accidents or deaths in a closed future [7].

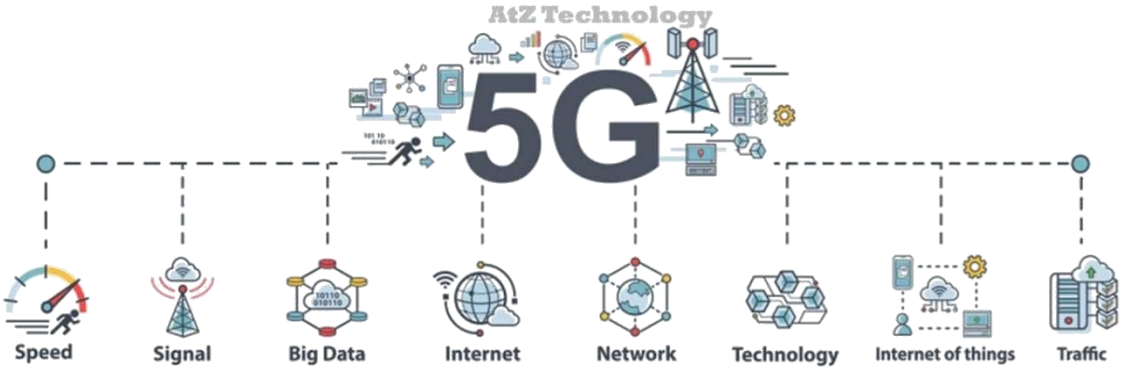

Figure 2. 5G Features [3].

1.2 – Motivations and objectives

Vehicle networks is seen as a key enabler for connected and autonomous driving, but were limited to increase the safety of road users and improve the traffic efficiency of roads [8]. However, the 5G New Radio (NR) V2X comes to support new applications, where ultra-low latency and very high reliability are required, and that can meet an end-to-end latency of 3ms and high reliability up-to 99.999% [9]. These requirements for both periodic and aperiodic traffics, as well as the half-duplex, and the hidden node problem are the main aspects for 5G-NR V2X physical layer design [10]. One of the main new features of 5G-NR V2X physical layer is the support to different subcarrier spacing associated to different frequency range, which enables robustness against Doppler [11]. However, there are studies on the impact of numerology on V2X Communications which claim that increasing subcarrier spacing involves a trade-off between the Inter Carrier Interference (ICI) and the Inter Symbol Interference (ISI) effects over the system performance [12].

In 5G-NR V2X, user equipment's (UEs) are vehicles, Road Side Units (RSUs), or mobile devices that are carried by pedestrian [13], which brings us to four different types of V2X communications: Vehicle-to-Vehicle (V2V), Vehicle-to-Infrastructure (V2I), Vehicle-to-Pedestrian (V2P), and Vehicle-to-Network (V2N)[14]. One or a combination of V2V, V2I, V2P and V2N may be applied to each use case, which are divided in the following four groups [15]:

- Vehicles Platooning: It supports the formation of an interconnected group of vehicles which exchange information to get shorter distances and fuel saving for platoon.
- Driving: It enables the semi-automated or fully automated driving, where each vehicle and/or RSU shares data obtained from its local sensors with surrounding vehicles in proximity, to coordinate their trajectories or manoeuvres, which increases the safety, avoids collisions, and improves the traffic efficiency.

- Extended Sensors: It allows to improve the perception of the environment beyond the perception capabilities of the drivers, through the collection of information by local sensors present in vehicles, RSUs, mobile devices of pedestrians, or V2X application servers.
- Remote Driving: It allows to control vehicle driving remotely, for dangerous and severe conditions, or for passengers who cannot drive themselves, whether by humans or cloud and edge computing applications.

The 3rd Generation Partnership Project (3GPP) standard defines two frequency bands as the operating bands for V2X: 5.9 GHz band (n47) and 2.5 GHz band (n38), where the supported channel bandwidth in both frequencies are 10, 20, 30, and 40 MHz [16]. Both frequency bands belong to Frequency Range 1 (FR1) ranging from 410 MHz to 7125 MHz, and therefore none belongs to the millimetre Wave (mmWave) Frequency Range 2 (FR2) yet, ranging from 24.25 GHz to 52.6 GHz [16]. Resource allocation in these bands for 5G-NR V2X is defined in two modes: Mode 1 and Mode 2 [15]. In Mode 1, the vehicles are covered by one or more base stations, and they are the ones which proceed to configured or dynamic scheduling of resources. In configured scheduling, resource allocation is based on pre-defined bitmap, while dynamic scheduling is performed every millisecond based on the varying channel conditions. In Mode 2, the UE is out-of-coverage and autonomously selects the resources from a preconfigured resource pool. The sensing-based semi-persistent transmission mechanism is quite explored, however, long intervals with the same allocation may result in persistent collisions, which reduces safety due to consecutive packet losses [17].

Currently, the implementation of V2X services is still in the embryonic stage with multiple pilots taking place in Europe, for example through the C-Roads platform, where the Allbesmart participates in partnership with the concessionaire of the A23 and A4 motorways, the company Globalvia. Therefore, this work aims to fill some of the gap on this area and design an effective PSCCH searching algorithm for 5G-New Radio (NR) V2X sidelink communications. This one can be applied either at the transmitting User Equipment, when decoding the PSCCH to discover the available resources, or at the receiving UE. To the best of our knowledge PSCCH searching algorithms, beyond the blind convention algorithm discussed in [13], specifically designed for 5G-NR V2X sidelink communications have not been addressed in the literature, yet.

Thus, the main specific objectives of this work include:

- Expose the requirements of vehicular radio communications for services of autonomous driving.
- Expose the 3GPP radio standard used in 4G and 5G vehicle communications.
- Implementation of vehicle-to-vehicle (V2V) radio communication protocols and analysis of their performance in different scenarios.

- A correlation analysis is performed to verify the peak values of the correlation of the received signal with the PSCCH DMRS, and the predominance of the desired peak over the others.
- Design an efficient algorithm to search/decode the Sidelink Control Channel for V2X sidelink communication systems.
- Finally, a theoretical runtime analysis is performed to compare the runtime of the proposed algorithm with the blind algorithm.

The communications protocols and the algorithms are implemented in MATLAB and evaluated under the 5G New Radio (NR) specifications [18].

1.3 – Contributions

The main contributions of this paper are the following:

- A correlation analysis is performed to verify the peak values of the correlation of the received signal with the PSCCH DMRS, and the predominance of the desired peak over the others.
- Based on the previous results, it is designed an efficient algorithm to search/decode the first stage SCI in 5G-NR V2X sidelink communication systems.
- Finally, a theoretical runtime analysis is performed to compare the runtime of the proposed algorithm with the blind algorithm.

The main findings of this work were submitted for publications in the following journal.

> R. Magueta, J. Domingues, A. Silva, and P. Marques, "Effective PSCCH searching for 5G-NR V2X sidelink communications", submitted to Electronics, SI "V2X Communications for Connected Vehicles", October 2021.

1.4 – Outline

This dissertation is organized into five chapters, which include the introduction of mobile communication system and their evolution throughout the years, a study about the vehicular communications, the description of the proposed algorithm for effective Physical Sidelink Control Channel (PSCCH) searching, the conclusion and future work.

In Chapter 2 is given a brief resume of the 5G, factors that drives the improvement of the wireless networks, the key technologies that enable the 5G and finally some 5G indicators. Discussing about the 5G use cases, the 5G standardization. Finally, it will be shown and explained how the architecture network is stablished, as well as probed with the radio protocol.

In Chapter 3 of this dissertation, it is referenced the kinds of vehicular communications, introduction to the evolution of cellular communications V2X, and exemplification o the Physical

layer structure of the NR-V2X. The importance of the MIB and how the information, SCI is transported in the Transport Block (TB). How the resources are allocated, finally, will be defined the Main differences between LTE-V2X and NR-V2X.

In Chapter 4, we present in detail the proposed PSCCH searching algorithm for 5G-NR V2X sidelink communications. We start by analysing the conventional decoding algorithm of the PSCCH, already implemented in MATLAB. Throughout some evaluation we realized that this algorithm is inefficient to searching the PSCCH, since all the processing should be done several times before successful decoding it. Therefore, we designed an eficient search/decoding algorithm based on the correlation of received signal with Demodulation Reference Signal (DMRS). Finally, the proposed algorithm is evaluated against the standard one.

In the final chapter of this dissertation we point out the main conclusions of this work and discuss some future work that could be done to improve the developed one.

Chapter 2 – Brief overview about 5G

In this chapter a brief overview about 5G, will take place, namely, the factors that drove the improvement of the wireless networks, some key technologies that enable the 5G, such as the mmWave, mMIMO, and small cells technologies. Some 5G indicators that suggest how the network is suitable are also presented, such as performance, efficiency, and growth indicators. It is presented the 5G use cases and explained how the 5G should be helpful in the future smart cities. Also, the vehicular communications, and the 5G standardization, with the principal release standards by the 3GPP are described. Finally, the network architecture is explained, as well as the radio protocol, and the 5G-NR physical layer, which is in focus in this dissertation.

2.1 – Factors driving the need of improved wireless networks

There are some factors that are driving the need for improving the wireless networks, such as more people requiring more data on more devices, the increasing total number of internet-connected devices, both consumer industrial devices and the industries depending on internet-connected devices every day because of business operations [19].

1) The first factor mentioned above is based on the simple fact that since 2016, more people in the whole world have been using more data on mobile devices, such as smartphones, than on their personal computers. It is expected that the mobile data traffic increases about seven times more from the year of 2016 to this current year, because the need of high-quality and high-demand video to mobile devices. The spectrum that is used for mobile communications is becoming crowded and congested as so, current networks, such as 3G and 4G LTE, cannot always answer to consumer demands for data, especially during periods, like emergencies, of heavy use. Because of these previous reasons, during periods of heavy use, consumers may experience slow speeds, unstable connections, delays, or loss of service.
2) The second factor is referred to market research that indicates in 2018 there were 17.8 billion connected devices globally, 7 billion of which were not smartphones, tablets, or laptops, but other type if connected devices, such as sensors, smart locks, that allow users to monitor and manage activities through a mobile device, like a smartphone. Because of this research we can expect an exponential increasing of the total number of internet-connected devices, both

consumer devices, such as smartwatches, smart meters, and some industrial devices like sensors that assist with predictive maintenance. This large number of connected devices worldwide will further increase the request on the network, therefore it is crucial to improve the wireless networks.

3) Finally, the third factor reports to the fact that the industries nowadays are dependent on internet-connected devices in everyday business operations, companies use devices to track assets, collect performance data, and inform business decisions. These devices, when connected, englobe the so called, Internet of Things (IoT), which is the collection of physical objects, for example health monitors, industrial sensors, that interconnect to establish networks of devices and systems that can collect and compute data from many sources. More advanced IoT devices, such as autonomous cars and emergency medical systems, need networks that can provide a persistent continuous internet connection. In other words an always-on connection, with low latency services, meaning a minimal lag time on commands, along a greater capacity, such as bandwidth, to access and share more data, and the ability to quickly compile and compute data [19][20].

Wireless networks are not the only ones that needs improvement, V2X also have this need. We can compare it with the necessity of transforming our cities in safer environments with less mortalities. This is possible if we improve the abilities to communicate between vehicles and pedestrians which could decreased the number of car accidents per year. Vehicle-to-pedestrian (V2P) is a sub communication that belongs to the V2X. This allows the communication between vehicles and pedestrians for example when someone is crossing the street, they can do it safely and without inducing a car accident if there is good communication. Another type of communication is vehicle to infrastructure (V2I) which allows vehicles to communicate with infrastructure around them. Two examples of this are traffic lights that are used in order to control speed and devices to advice highway users to be aware of weather measurements to prevent possible accidents[17].

Succinctly, the features that current mobile network cannot consistently support as well the urging of this vehicular communications supported by the V2X, implies the need to improve the current wireless network [19][20].

2.2 – Key enabling technologies of 5G

Nowadays, with the increasing demand of higher data rates in future wireless networks, researchers have been considered an enabling technology to achieve the large deployment of the number of antennas with the access to more bandwidth. For these reasons the emergence of some technologies, like the mMIMO, mmWave, and finally the small cells, for ultra-dense networks, should propel the revolution on the 5G wireless network technology.

These technologies are the three pillars that allow 5G, as we can see in **Figure *3***, to achieve all requirements for the three main usage scenarios, the Enhanced Mobile Broadband (eMBB) , with a wide-area coverage and hotspots for a high capacity and flawless user experience, Ultra-Reliable and Low Latency Communications (URLLC), Massive Machine Type Communications (mMTC), with a very large coverage and number of connected low-cost devices employing a very long battery life [21][22].

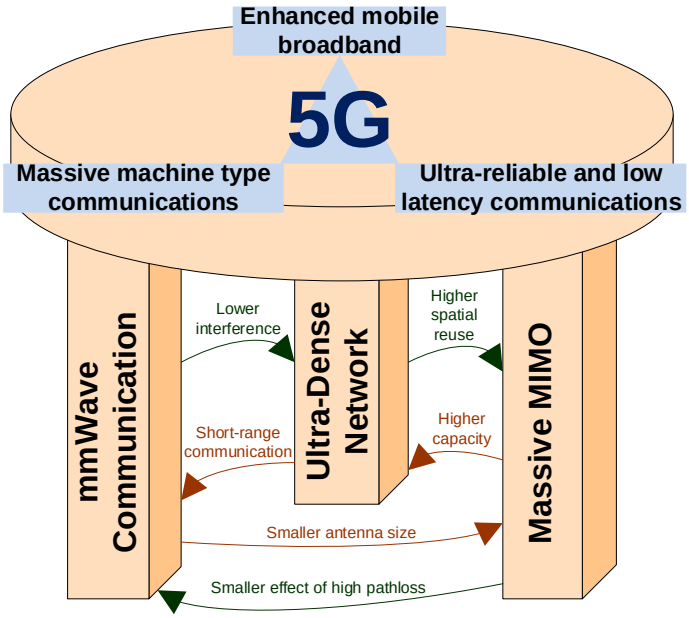

Figure 3. Key Enabling Technologies of 5G [15].

2.2.2 – Massive MIMO

The decrease in wavelengths of the mmWave leads to the decrease of the antenna's size and enables the possibility to deploy massive MIMO (mMimo) systems, as is illustrated in **Figure *4*.** mMIMO system [24].Such as a scaled-up MIMO by orders of magnitude compared to the conventional MIMO approaches, by decreasing in the space between antennas. The use of mMIMO can improve the efficiency of the bandwidth but also the reliability through enhancement the multiplexing gains or whether the diversity gains with that the inherent high Degrees of Freedom, DoF. This one is convenient to implement a high spatial reuse, allowing the reduction of the multi-user interference by directing energy only to the defined terminals and boosting the overall ultra-dense network capacity, with narrow beams that can be obtained with many antennas. More than ever, mMIMO is each more robust against fading, the failure of antenna units and it reduces the constraints on accuracy and linearity of each individual amplifier [23][24].

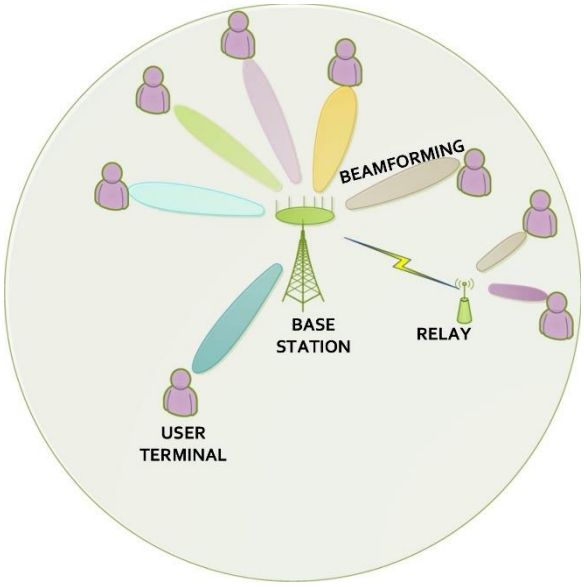

Figure 4. mMIMO system [24].

2.2.1 – Millimetre-wave

The mmWave has a frequency spectrum compressed from 30 to 300 GHz, represented in the following **Figure 5**, corresponding to wavelength from 1 cm to 1 mm, and this band's use is intended for the future of mobile communications. This feature allows a better data rate in the order of Gb/s, which can be a support for many applications such as short-range communications, vehicular networks, and wireless backhauling [25].

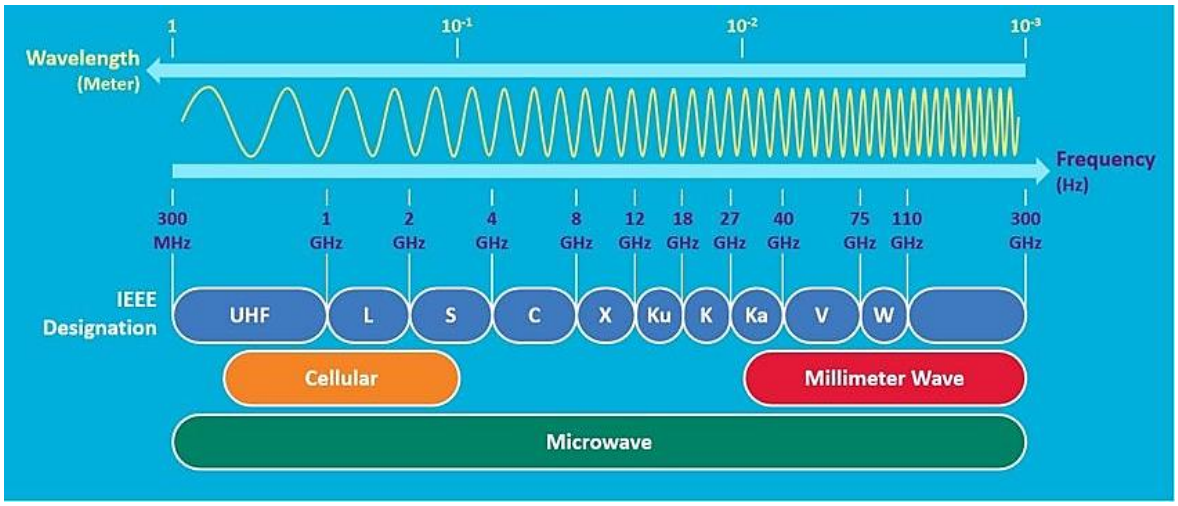

Figure 5. MmWave spectrum band [17].

This technology is not highly complex however, a problem occurs because at high frequencies, the communication between base station and the user terminal must be in or near line of sight, LOS. This problem appears because higher frequencies generate more path losses and attenuation than the current used frequency spectrum. Moreover, the mmWave spectrum had some

attenuation in some specific bands, like the oxygen absorption, between 57 GHz and 66 GHz and from water vapor absorption, between 164 GHz and 200 GHz, like we can see from the **Figure 6**,

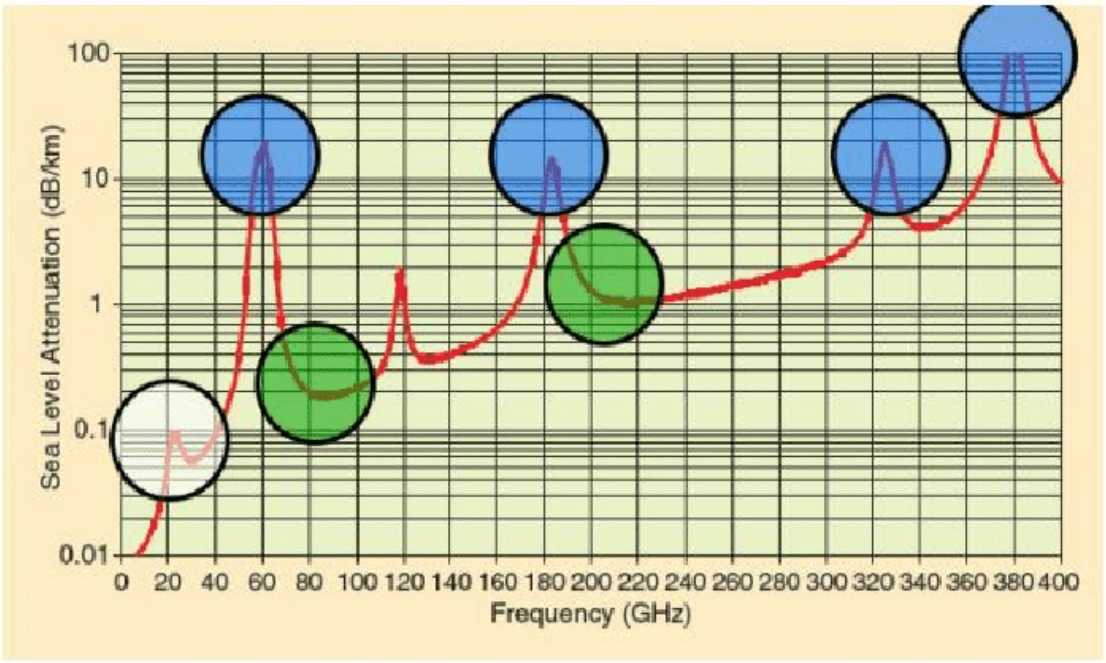

Figure 6. Attenuation in mmWave band [18].

For mmWave is hard to cross walls, glass as other objects described in the **Table *1***,

Table 1. mmWave attenuation values in dB for different materials [16].

MATERIAL	THICHNESS(CM)	< 3 GHZ [26] [27]	40 GHZ [28]	60 GHZ [26]
DRYWALL	2.5	5.4	-	6.0
OFFICE WHITEBOARD	1.9	0.5	-	9.6
CLEAR GLASS	0.3/0.4	6.4	2.5	3.6
MESH GLASS	0.3	7.7	-	10.2
CHIPWOOD	1.6	-	0.6	-
WOOD	0.7	5.4	3.5	-
PLASTERBOARD	1.5	-	2.9	-
MORTAR	10	-	160	-
CONCRETE	10	17.7	175	-

Because of this high attenuation with distance, like described before and as we can see in the **Table *1***, this technology enables the use of the small cells which are based network, to reduce the interference between those cells. Also, as mmWave is considered short-range waves, the combination of mmWave and the densification of small cells in the macro cells is a promising solution to improve the available data rate and system capacity for the future generations of mobile communications [25].

2.2.3 – Small cells

Following up we have other technology, that is the small-cell, which it is schematized into the **Figure *7***, and in this context could bring some advantage, such as less cost and less power usage, because since low-cost power components can be used, as well as expensive and bulky components as large coaxial, and high-power radio frequency (RF) amplifiers at the front-end can be eliminated. Moreover, the small cells allow to prolong the battery life of each device, decreasing the energy consume, and then, the devices can be more time connected without need a charge up.

The main 5G tower, with high structures and power that can keep the signal strong for big distances, the small cell adapts in scenario with a larger population density and some physical barriers, like cities. The main goal of this technology is amplifying the cellular experience, like

mobile data, for the final user which will use the 5G enabled smartphones, enhancing the mobile data coverage and the transfer ratio of data, where competition between devices for bandwidth exist.

Finally, there are some challenges in small cells that should be noted, namely there is a probability of taking too long and it being too expensive to deploy this technology, because of identification of the millions of necessary locations, acquiring permits for identified locations, and some operational costs to lease, deploy and maintain sites for most of these small new cells [29].

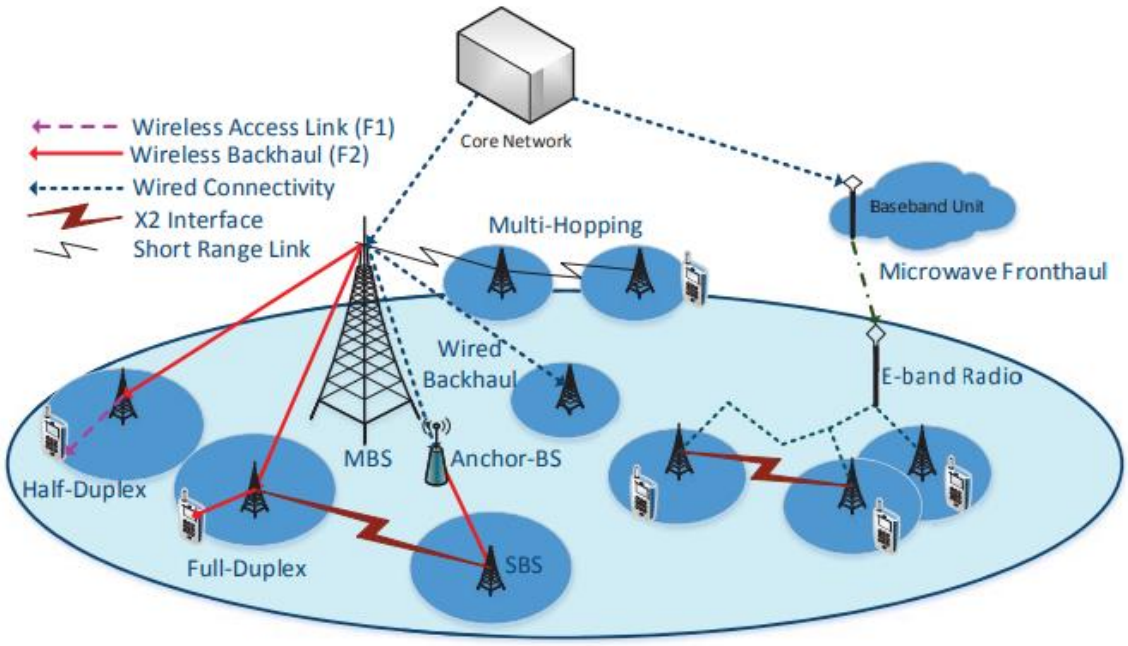

Figure 7. small cell system [26].

2.3 – 5G Indicators

The appearance of this new generation in mobile networks, the 5G, brings the emerging of some indicators, like growth, efficiency, and performance indicators.

In terms of growth indicators:

- the total number of subscriptions to 5G networks, for example pre-paid active SIM cards, for voice and data information transfer between two humans, H2H, but the communication between two machines, M2M and finally the communication between a machine and a human being, implying a single subscription for multiple devices.
- the number of 5G connected devices, including the communications between humans, machines, and devices, giving a single device some subscriptions.

- The total percentage of population that have 5G coverage, whether are subscriber or not, in relation to the total of population, giving an idea of the ratio between the population covered by 5G signal and the total number of populations in a respective area.
- the total percentage of land that have 5G coverage, in relation to the total of land that is in analysis, giving an idea of the ratio between the land covered by 5G signal and the area total that is being evaluate.
- the total percentage of devices connected by 5G network, like human and machine communications, in relation to the total of population that is in analysis, giving an idea of the ratio between the number of devices connected into 5G network.
- the number total of population and the total percentage of devices connected by 5G network, resulting the ratio between the total number of devices into the 5G network and the total number of populations in some area that is being tested.

In order of efficiency indicators:

- like the data throughput per unit of spectrum resource per area unit, the Spectrum efficiency.
- the number of bits that can be transmitted per unit of cost, the Cost efficiency.
- the number of bits that can be transmitted per joule of energy, the Energy efficiency.

Finally, the performance indicators:

- minimum that is possible achieved data rate for each user in the real network environment, User experienced data rate in bps.
- the number of connected devices in each area, the connection density.

- the total data rate of all users in each area, the traffic volume density in bps/km2, the speed relative between the receiver and the transmitter under certain performance requirement.
- the mobility in km/h, the maximum data rate that should be achieved for each user, the peak data rate into bps.
- the delay from the time that a packet is sent from the transmitter until the same is received at the receiver that is called the latency [20].

2.4 – Use of 5G Technologies

Consumers are able to download a full-length, high-definition movie on their mobile device in a matter of seconds, can join in video streaming without a single interruption, finally they will have the opportunity to participate in online gaming anywhere. These 5G technologies are expected to create new type of revenue streams for technology companies and telecommunications providers.

5G technologies are also expected to support interconnected devices, like for example smart homes, medical devices, and advanced IoT systems, such as autonomous vehicles, precision agriculture systems, industrial machinery, and advanced robotics. IoT technologies are expected to be integrated into industrial systems to automate procedures and to optimize operational efficiencies.5G networks are expected to support the growing IoT industry, enabling device makers to develop and deploy new IoT devices and systems across multiple industries, and sell IoT products globally, yielding significant economic gains for technology companies and for the countries where those companies are located, these technologies are schematized into the following **Figure 8**[20].

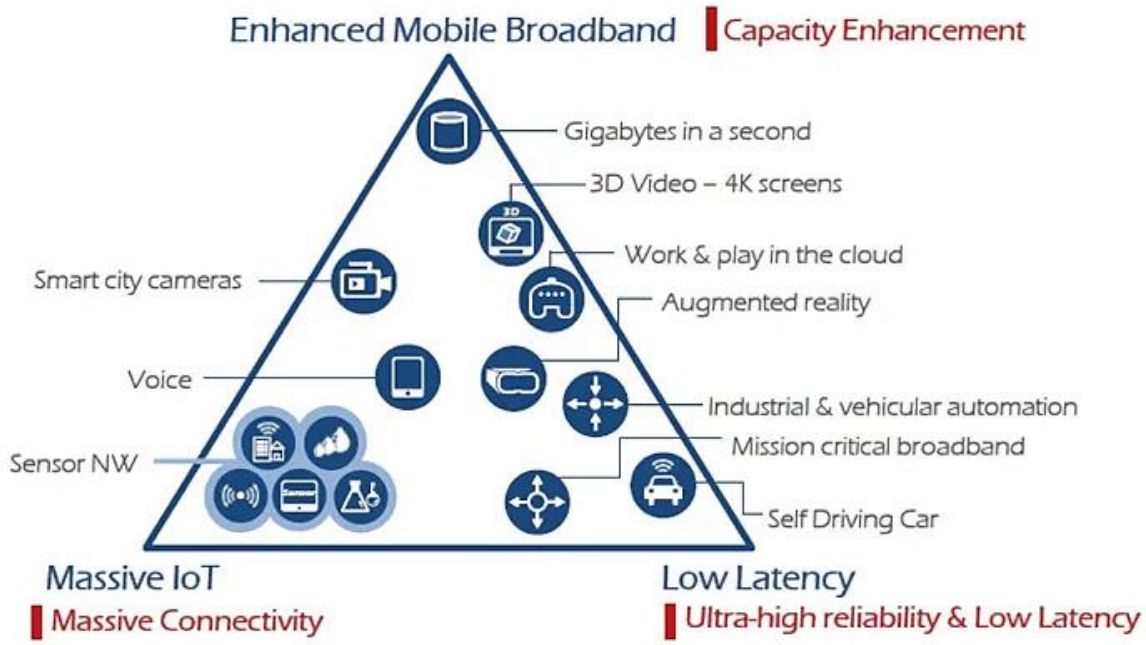

Figure 8. Use of 5G Technologies [11].

2.5 – Standardization

The evolution from the 3G, The Universal Mobile Telecommunications System (UMTS), troughing the 4G LTE and 5G, will bring to us the IoT, along with others features, phased into some releases like the release 15, that finished in June of 2019, defining a new cellular network, based on microservices and Service-Based Architecture (SBA). Release 16 that finalized in July of 2020, was focused in the 5G system expansion, such as, the introduction of the definition from the prioritized multimedia service, some services from the applicative layer V2X, 5G satellite access, local network 5G access, between others.

These releases are exposed in the following **Figure *9***,

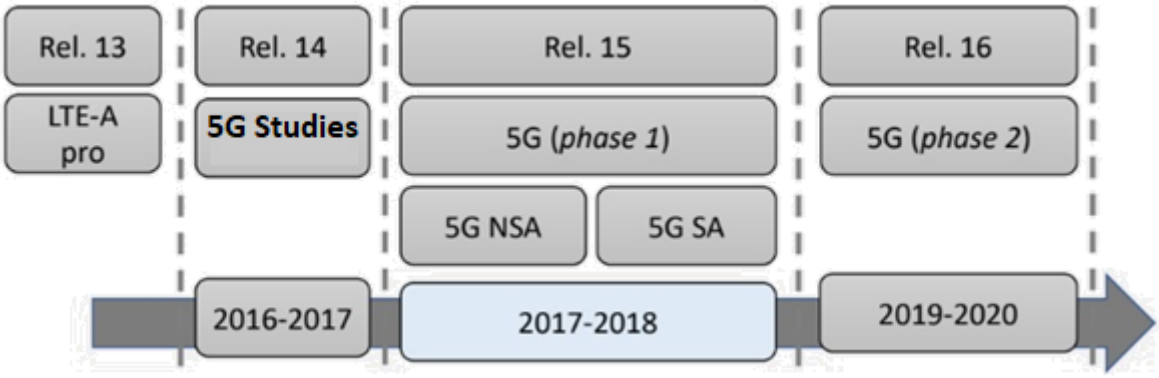

Figure 9. 5G releases [27].

Although sidelink transmissions in Release 12 enable UEs that cannot be served by eNBs (known as out-of-coverage UEs) to directly exchange messages, it is still highly desired to access the network if eNBs are available. In this case, it is feasible to extend the service range of an eNB with the facilitation of UEs that can be served by an eNB (known as in-coverage UE). To this end, sidelink transmissions in Release 13 support UE-to-Network relay, in which an in-coverage UE is able t relay signals between an eNB and an out-of-coverage UE. To avoid significant impacts on the operations of Release 12 sidelink transmissions which have been deployed, a lot of countries that deploy Release 12 as their public safety networks also decide to keep the interface of sidelink transmissions unchanged. Under this constraint, Release 13 sidelink transmissions reuse all the Layer 1 and Layer 2 functions of Release 12. However, only Layer 1 and Layer 2 functions are insufficient to support the UE-to-network relay, and additional procedures on the top of Layer 1 and Layer 2 (i.e., Layer 3) are required. As a result, the UE-to-network relay in Release 13 is a Layer 3 based relay.

In Release 14, the scenario of sidelink transmissions is extended from D2D ProSe solely for public safety to V2X, in which the major services include the cooperative awareness message (CAM) and the decentralized environmental notification message (DENM) exchanges among vehicles, pedestrians, and infrastructures, for other words eNBs or road-side units, RSUs. Observing the fact that these services also rely on broadcasting transmissions, most functions of sidelink transmissions in Release 12 can also be adopted in Release 14. Nevertheless, consider that the CAM and the DENM require low-latency transmissions, and the connection density in V2X is also higher than that in public safety. Hence, some functions in Release 12 sidelink transmissions should be redesigned, such as the multiplexing scheme for radio resources of the physical sidelink control channel (PSCCH) and physical sidelink shared channel (PSSCH). In addition, the capability of channel sensing (not supported in Releases 12 and 13 is introduced to Release 14 sidelink transmissions to avoid resource collisions among UEs.

In Release 15, the 3GPP continues the evolution of Release 14 sidelink transmissions, and new functions such as carrier aggregation (CA), transmission diversity, and 64 quadrature amplitude modulation (QAM) are adopted to further enhance the throughput and reduce the latency.

In Releases 12 to 15, sidelink transmissions are designed based on the air interface of LTE-A, which however may not fulfil the service requirements imposed by the International Mobile Telecommunications-2020 (IMT-2020). To migrate to the fifth generation (5G) network, 3GPP subsequently launched the standardization progress of NR sidelink transmissions in Release 16. Although the major scenario of Release 16 NR sidelink transmissions also targets at V2X, the services are no longer limited to the CAM and the DENM. Instead, sustaining the next generation driving use cases (including advanced driving, vehicle platooning, extended sensors, and remote

driving) are the major goals. These use cases demand low-latency, high reliability and high-throughput transmissions, as well as a high connection density. To fulfil these new requirements, four new designs are particularly introduced to NR sidelink transmissions. Not only broadcast but also unicast and groupcast are supported in sidelink transmissions. For unicast and groupcast, the physical sidelink feedback channel (PSFCH) is newly introduced for a receiving UE to reply to decoding status to a transmitting UE. To improve the latency performance, grant-free transmissions that are adopted in NR uplink transmissions are also provided in NR sidelink transmissions. In order to alleviate resource collisions among different sidelink transmissions launched by different UEs, it enhances channel sensing and resource selection procedures, which also lead to a new design of PSCCH. To achieve a high connection density, congestion control and thus the QoS management is supported in NR sidelink transmissions.

The technical specifications (TS) for 5G-NR are shown in **Figure 10**,

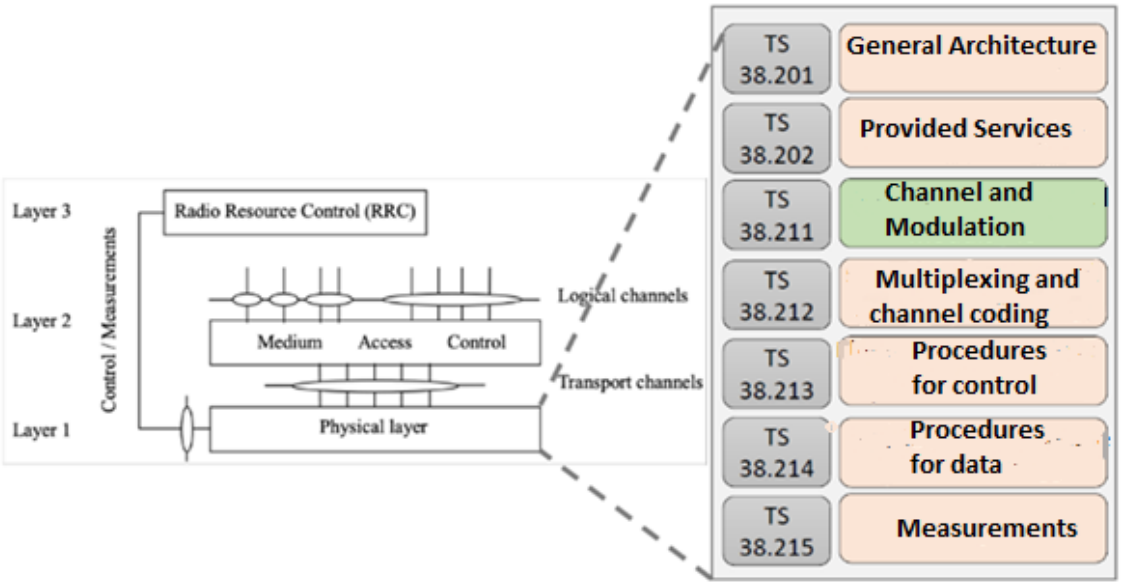

Figure 10. Standardization of the physical layer [27].

2.6 – Network architecture

Alongside with the specifications of the network architecture from the 5G NR, 3GPP members have worked together to develop, test, and build specifications for 5G technology. In December 2017, 3GPP approved the "non-Standalone version of the New Radio standard" allowing carriers to supplement existing 4G networks with 5G technologies to improve speed and reduce latency the need of support the existing 4G LTE networks on the 5G NR, Non-Standalone (NSA). In June 2018, 3GPP completed the "Stand-Alone version of the New Radio standard." This specification supports the independent deployment of 5G NR, using core networks that are designed to support advanced IoT devices and functions.

The 5G NR access network using the NR Stand-Alone (SA), i.e., a network where is used the 5G core, are standardized by the 3GPP, Meanwhile, exist non-3gpp access networks, which access points to the UE are not trustable by the mobile operator, that means the device it is connected. An example of a SA network is shown in **Figure 11**, because, as we can see, the radio access network (RAN) is connected with 5G-Core using the control and user plans. The user plan is connected to the Data Network (DN), from where we can get data information to transfer. Finally, 3GPP and non-3GPP can connect to the radio access network (RAN).

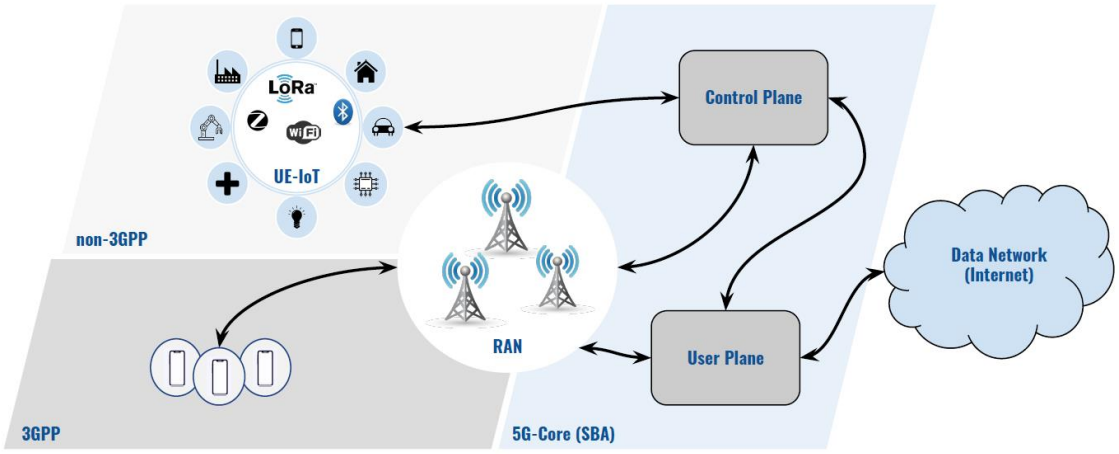

Figure 11. general network architecture [30].

The **Figure 11** shows an overview of a 5G network, where we can identify:

- The RAN composed by antennas, radios and baseband units.
- The 5G core composed by
  - Unified Data Management (UDM)
  - Policy Control Function (PCF)
  - Network Exposure function (NEF)
  - Application Function (AF)
  - NRFNF Repository function (NRF)
  - Unified Data Repository (UDR)
  - Access and Mobility Management function (AMF)
  - Session Management function (SMF)
  - User plane function (UPF)
- And the UEs. The UE-A and UE-D are connected to RAN and can perform the downlink and uplink. The communication between UE-A/ UE-D, and between UE-

A/ UE-B is sidelink Mode 1. Finally, the communication between UE-B/ UE-C is sidelink Mode 2. The difference of Mode 1 and 2 is explained in subchapter 3.5.

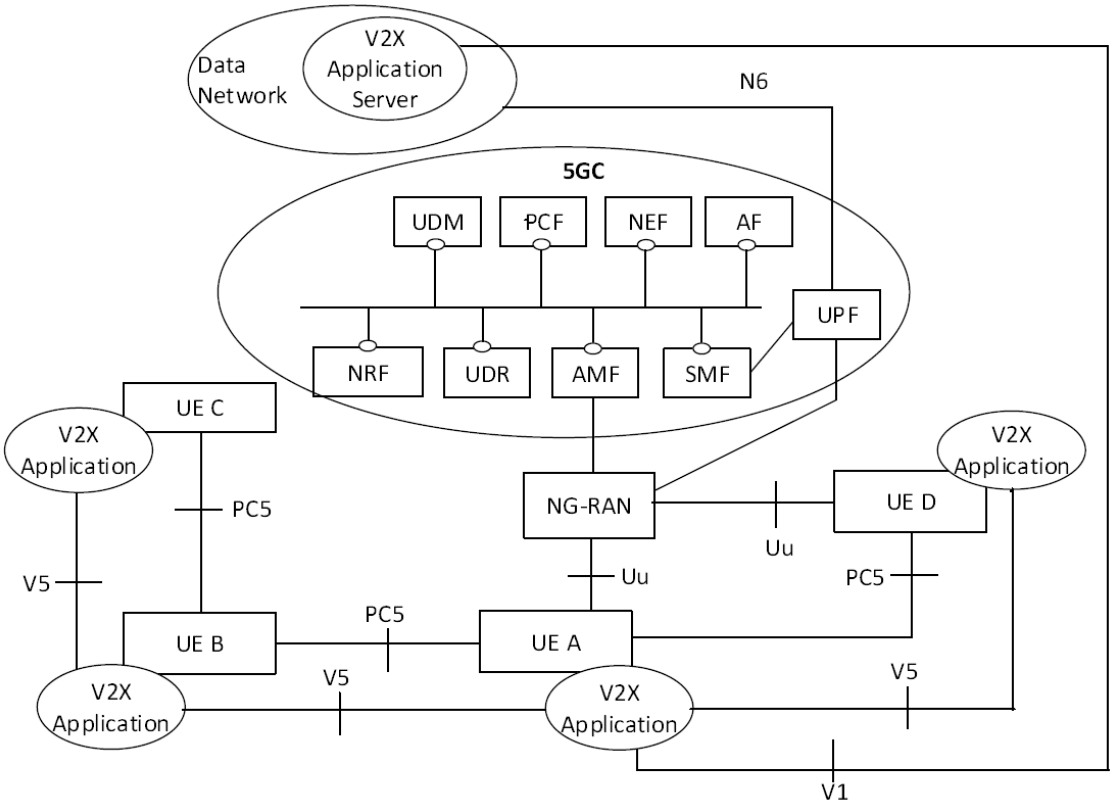

Figure 12. Network architecture [29].

2.7 – Radio protocol stack

Despite the previous topic was talking about the 5G general network architecture, the attention of this document is talk and describe the 5G layer 1, the of the so-spoken physical layer. The Physical Layer is contained by two different and distinguished plans, the User Plane Protocol Stack, also known as U-Plane Protocol Stack, and Control Plane Protocol Stack, also called as C-Plane Protocol Stack, represented in the **Figure *13***. In the **Figure *13*** there is an overview of both, with the blocks associated to each of them [31].

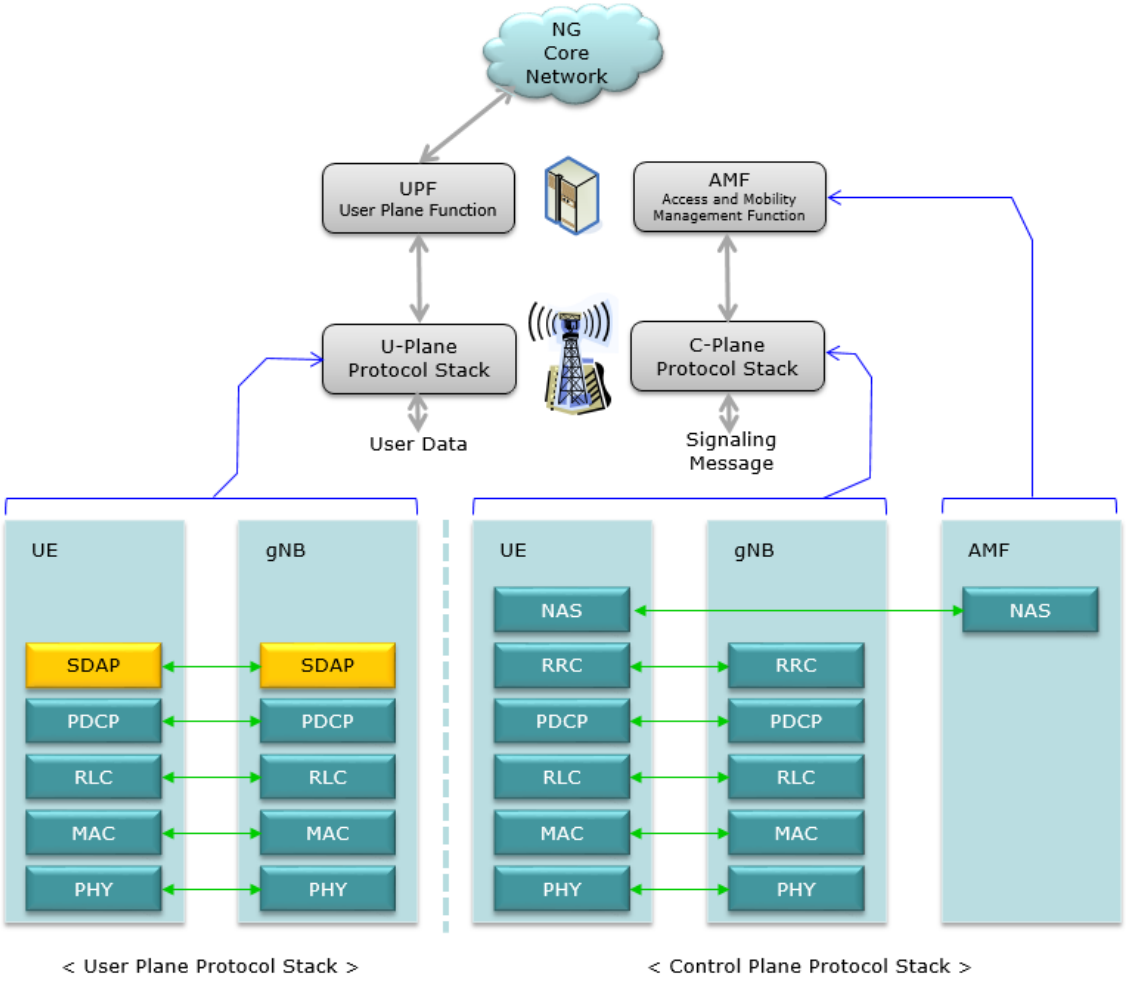

Figure 13. User Plane and Control Plane Protocol Stack [30].

Giving a simple example from the U-Plan Protocol stack, such block is decomposed as the follow **Figure 14** represent,

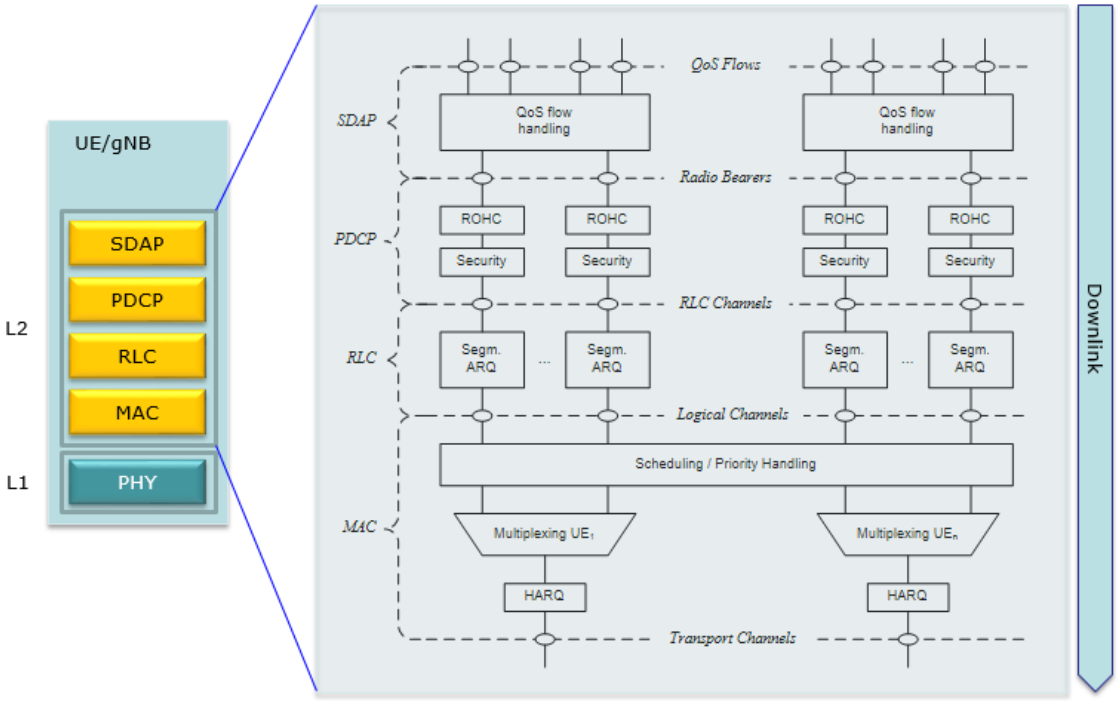

Figure 14. Layer 2 schematized [30].

The physical layer (PHY) offers a transport channel to MAC and data transport services to higher layers, The access to these services is using a transport channel via the MAC sub-layer. The multiple access scheme for the NR physical layer is based on OFDM with a CP. The Layer 1 is defined in a bandwidth agnostic way based on resource blocks, allowing the NR Layer 1 to adapt to various spectrum allocations. A resource block spans 12 sub-carriers with a given sub-carrier spacing [32].

The MAC sublayer provides data transfer services on logical channels. To accommodate different kinds of data transfer services, multiple types of logical channels are defined, in other words, each supporting transfer of a particular type of information [33].

The RLC is a layer 2 Radio Link Protocol used in 5G on the Air interface. This protocol is specified by 3GPP 5G NR, and it is located on top of the 3GPP MAC-layer and below the Packet Data Convergence Protocol (PDCP)-layer. The main tasks of the RLC protocol are for example, Transfer of upper layer Protocol Data Units (PDU) in one of three modes, Acknowledged Mode (AM), Unacknowledged Mode (UM) and Transparent Mode (TM) and has task to protocol error detection and recovery[34].

The PDCP is specified by 3GPP for 5G NR, and it is located in the Radio Protocol Stack in the 5G Air interface on top of the RLC layer. Provides its services to the Radio Resource Control (RRC) and user plane upper layers, for example the IP at the UE or to the relay at the base station.

The following services are provided by PDCP to upper layers, like the transfer of user plane data and the transfer of control plane data[31].

The Sublayer SDAP (Service Data Adaption Protocol) it is in air-interface protocols stack both at UE and the gNodeB (gNB) side. This one is the topmost L2 sublayer at 5G NR protocol SA where gNB connects to 5G Core network SDAP[35].

At this example we can see the Ue and the gNB, which have the same structure in terms of the user plan protocol stack, and we can distinguish the different sublayers from the layer 2, such as the MAC, RLC, PDC and the SDAP sublayer, in terms of downlink, and how these sublayers are decomposed.

In terms of 5G channels, we have the logical channels, which represents the type of information is transferred, the transport channels. It is basically how, with and which characteristic is transferred. Finally the 5G channels are shown in **Figure 15**.

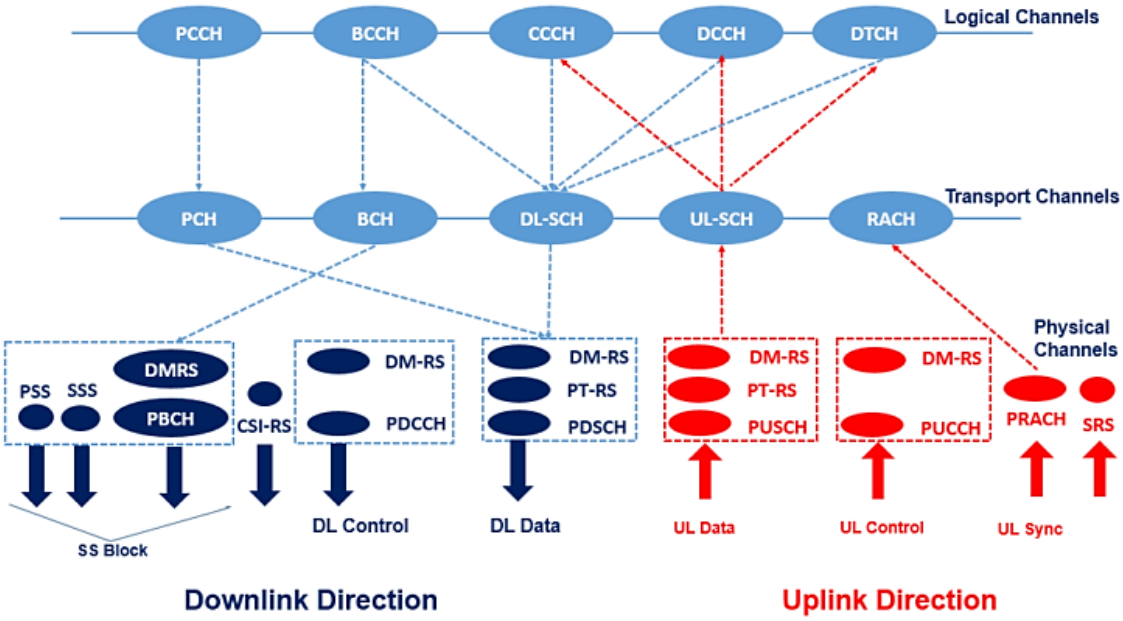

Figure 15. 5G Channels [35].

Chapter 3 – Vehicular communications

In this chapter will be referred the all kinds of vehicular communications from the 5G like the vehicle-to-vehicle (V2V) or the more generic V2X, between others, introducing the evolution of cellular communications from the D2D to the actual V2X.The exemplification of the Physical layer structure of NR-V2X, with it numerology, waveform and how the resource are structured in the time domain and in the frequency domain. The physical channels, like the PSSCH, the PSCCH between others will be explained but also the reference signals, which are very important too in this technology. How the information, Sidelink Control Information, the SCI, is transported and the importance of the Master Information Block, the MIB, which provides some important information like the system bandwidth, and it frame number and how the resource are allocated. Finally, it will be presented the main differences between LTE-V2X and NR-V2X.

3.1 – Kinds of vehicular communications

The 5G of cellular network can be considered the way to the pervasive Internet and persistent paradigm. The Internet of Vehicles (IoV) uses the network infrastructure to allow cars to be connected to new radio technologies, and it can be supported by 5G networks. In order of that, V2X integration needs 5G connections unavoidably.

Vehicular communications, those one is described in the **Figure 16**, require some wireless communication infrastructure to always have signal coverage. The 5G cellular network emerges as a new strong alternative to allow such connections, in a reliable, secure, and fast way, providing the IoV, as well as the V2X scenarios integration. It is expected that the 5G network can be able to attend the requirements for the future IoV applications and to offer ITS in several scenarios involving high mobility, dynamic network topology, and high data volume.

IoV can be considered part of intelligent cities and it is characterized as an open and integrated network system, composed by several components, including vehicles, people, and things, as the **Figure 16** illustrates. It shows that there are six V2X application types divided into these two basic operations, D2D involving the V2V, the V2I, the V2P and the Vehicle-to-Network (V2N) with evolved packet switching communications. Also, the communications between the vehicles are also

a type of vehicular communications, V2V, and the communications between the vehicle-to-the grid (V2G). In this ecosystem, safety enhancement V2X (eV2X) services or scenarios include automated driving, vehicle platooning, extended sensors, and remote driving. However, mobile entertainment with high data rate is an example of non-safety for V2X scenarios [13][36].

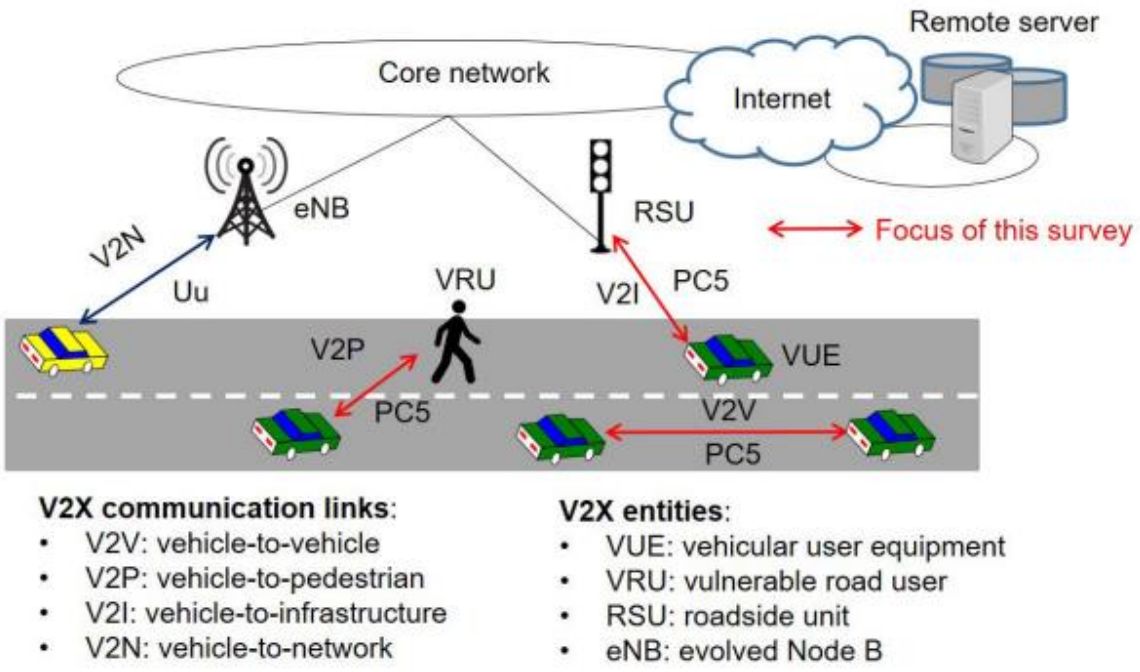

Figure 16. Kinds of vehicular communications [12].

3.2 – Evolution of cellular V2X

The Cellular Vehicle-to-Everything (C-V2X) is a state-of-the-art wireless technology used in autonomous driving and ITS. This technology has extended the coverage and blind-spot detection of autonomous driving vehicles. Economically, C-V2X is much more cost-effective than the traditional sensors that are commonly used by autonomous driving vehicles. This cost-benefit makes it more practical in a large-scale deployment. PC5-based C-V2X uses an RF sidelink direct communication for low latency mission-critical vehicle sensor connectivity. Over the C-V2X radio communications, the autonomous driving vehicle's sensor ability can now be largely enhanced to the distances as far as the network covers.

In 2020, 5G is commercialized worldwide, and Taiwan is at the forefront. Operators and governments are keen to see its implications in people's daily life brought by its low latency, high reliability, and high throughput. Autonomous driving class L3 stands for conditional automation or L4 meaning Highly Automation are good examples of 5G's advanced applications. In these applications, the mobile networks with are perfectly demonstrated. Therefore, C-V2X evolution and 5G NR

deployment coincide and form a new ecosystem. This ecosystem will change how people will drive and how transportation will be managed in the future

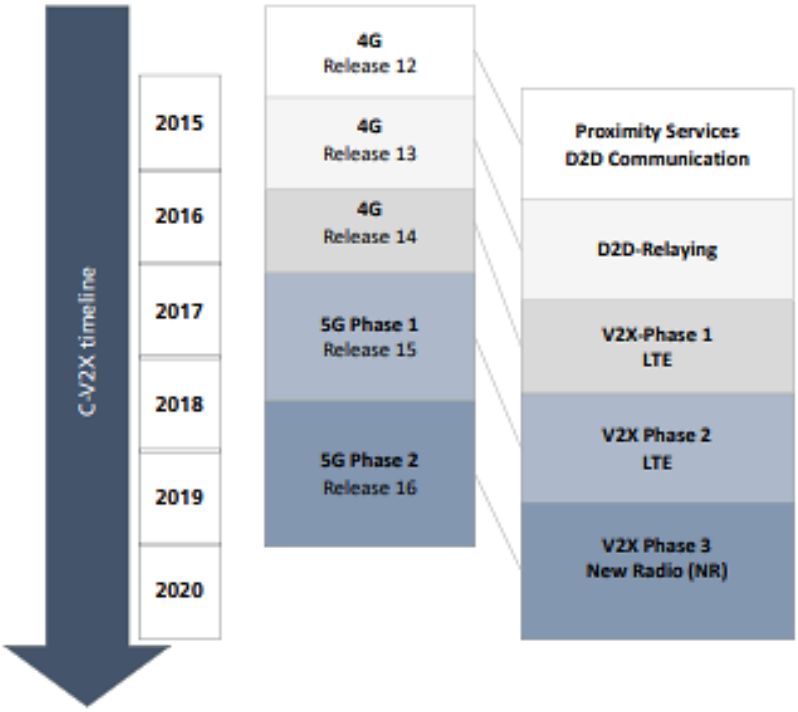

Figure 17. Evolution of cellular V2X [37].

With the evolution of Cellular V2X, C-V2X, the first phase, the phase 1 of 3GPP Release-14, was completed in March 2017, providing the initial standards supporting V2V services and the additional V2X services leveraging the cellular infrastructure. The primary safety features of C-V2X under 3sGPP Rel-14 were delivered through cellular networks or sidelink communications via the PC5 interface. A new LTE-V2X band 47, with 10 and 20 MHz bandwidth, was introduced to support C-V2X by unlicensed 5.9 GHz spectrum. 3GPP Rel-14 also introduced two new physical channels for PC5-based C-V2X communication, namely the PSSCH and the PSCCH. As the name discloses, PSSCH carries data, and PSCCH has control information for decoding the data channel in the physical access layer. To accelerate the LTE-V2X development, LTE-V2X uses the centralized scheduling mode, as mode 3, and decentralized scheduling mode, the mode 4, of LTE-D2D, supporting sidelink communications via PC5 interface. The cellular network allocates resources under Mode 3. On the other hand, Mode 4 does not require cellular coverage, vehicles can autonomously select their radio resources using a sensing-based Semi-Persistent Scheduling (SPS) scheme supported by congestion control mechanisms. In June 2018, 3GPP Rel-15 was completed. The enhanced V2X services such as platooning, extended sensors, advanced driving, and remote

driving were introduced as phase 2 of 3GPP V2X, which has formed a stable and robust ecosystem around LTE-V2X, as the **Figure *17*** illustrates.

Nowadays we are currently in the phase 3, that stars around the year of 2020, which has the main goal of the 3GPP release-15 with the plus of the enhancements and the new evaluation of the 5G new radio, 5G-NR, within the 5G services. The evaluation methodology consists in the sidelink communications above the 6 GHz spectrum and some new use cases that came with these communications[37][8].

3.3 – Physical layer structure of NR-V2X

The 5G has the novelty of supporting different numerologies. In this subchapter, it is presented the 5G-NR numerology, the waveform, and the structure of resources in time and frequency.

3.3.1 - Numerology

In order to achieve the specific peak data rate of about 20 Gbps , that it is a requirement required by the norm of IMT-2020, a better and larger bandwidth should by a needing, but, the so called differences of the allocation policies from the various countries, originate some sort of problems, that has been a worldwide challenge to identify which are the bands with enough bandwidth on the spectrum below from the 7 GHz, that it is known as the frequency range 1, FR1.

With this difficulty that emerge, the New Radio, NR, it is designed to be able for deploying in different carrier frequencies, including the FR1, already spoken before, together now with the spectra above the 7 GHz, also called as the frequency range 2, FR2. The result from this conjunction, is a signal propagation on different carrier frequencies that may suffer from different levels of multi-path fading consequently these different levels suffers also from the frequency selective fading.

With the main goal to easily the equalization performed at the receiver side, it is desired to deploy the so called orthogonal frequency division multiplexing, OFDM, where subcarriers has a smaller subcarrier spacing, SCS, for the spectra of a lower carrier frequency, while it is being deployed subcarriers with a larger SCS, in this way, for the spectra of a higher carrier frequency, at the end of this, these different SCS values are supported by New Radio.

On the other hand, those different values from SCS could be associated with other different values of cyclic prefix, CP, lengths for combat with different levels of inter-symbol interference, ISI, that are caused by multipath fading. The New Radio has these two types of Cyclic Prefix, caused by the different Cyclic Prefix length to symbol duration ratios, and for that there is the normal Cyclic Prefix, NCP, and the extended Cyclic Prefix.

In generally describing these different pairs of SCS values and CP types, the terminology known as numerology is adopted in NR. The NR sidelink transmissions support the following numerologies, For the FR1, the 15 kHz, 30 kHz, and 60 kHz SCSs with the NCP are supported, while the ECP can only be applied to the 60 kHz SCS. For the FR2, the 60 kHz and 120 kHz SCSs with the NCP are supported, while the ECP can only be applied to the 60 kHz SCS[38].

The following **Table *2***, which it is a combination from others tables[39] illustrates how the parameter numerology affects the subcarrier spacing, the OFDM symbol duration, the CP duration as well the OFDM Symbol including CP.

Table 2. Numerology [39].

PARAMETER NUMEROLOGY(μ)	**0**	**1**	**2**	**3**	**4**
SUBCARRIER SPACING (KHZ)	15	30	60	120	240
OFDM SYMBOL DURATION (μS)	66.67	33.33	16.67	8.33	4.17
CP DURATION (μS)	4.69	2.34	1.17	0.57	0.29
OFDM SYMBOL INCLUDING CP (μS)	71.35	35.68	17.84	8.92	4.46
$\mathbf{N_{symbol}^{slot}}$	14	14	14	14	14
$\boldsymbol{N_{slot}^{frame,\mu}}$	10	20	40	80	160
$\boldsymbol{N_{slot}^{subframe,\mu}}$	1	2	4	8	16

3.3.2 – Waveform

A few years ago, from now, in June from 2017, which has been marked has the early phase discussion about the 5G, one of the main topics of interest was, what kind of waveform should be used in the 5G, and because about that interest a lot of new ideas, new waveforms for this technology, emerge and were proposed.

In those discussion about which should be the correct waveform for the 5G, there is some technically problem that might exists, because some questions have emerged like, what is the problem in the current OFDM based waveform and why there is the need to redesign the waveform in 5G.However, the most recent discussion that started it is based in the sensing of the OFDM, would get more attention and finally as 3GPP specification rolls out, has been decided base the 5G waveform with the old and familiar waveform from OFDM.

In summary this waveform might be a little bit disappointing to those who have been expecting a completely new technology, in other words a disruptive technology, but for the studies

involving the 5G, and more concrete on this dissertation, this type of based waveform has some credit and truly and satisfactory[40].In the following schematic, represented in the **Figure *18***, shows overall flow of waveform generation for sidelink, which one uses CP-OFDM,

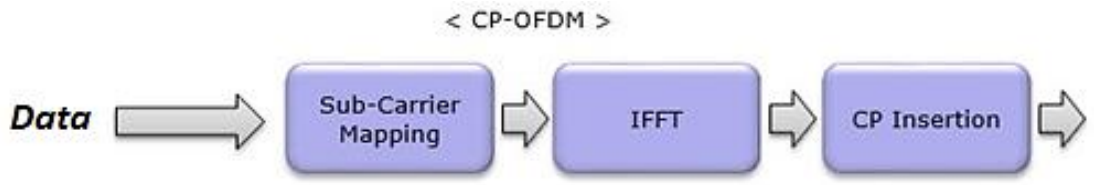

Figure 18. Waveform Generation [34].

3.3.3 – Resource structure in the time domain

In the NR, the resources belonged to the time domain are formed by some components like the following:

- the frame is fixed to 10 ms being composed by 10 subframes.
- in the Subframe is fixed to 1 ms,
- the slot is composed by 14 OFDM symbols in the case of Normal Cyclic Prefix (NCP) and it is composed by 12 OFDM symbols in the case of Extended Cyclic Prefix (ECP). Also, the length of each slot depends on the adopted SCS value, in the 15 kHz SCS, the length of a slot is 1 ms, which is exactly the length of a subframe, in the other side the 30 kHz, the 60 kHz, and the 120 kHz SCSs, the lengths of each slot are 0.5 ms, 0.25 ms, and 0.125 ms, respectively. Finally,
- Finally, there is the mini-slot, that the main aspect is that to further shorten the latency in uplink and downlink transmissions, mini-slots are further supported by NR. Each mini-slot is composed of 2, 4, or 7 OFDM symbols, depending on practical configuration, therefore NR sidelink transmissions, mini-slots are not supported, and the minimum unit for the resource scheduling in the time domain is a slot. However, the partial slot transmission for sidelink is supported in case that only some of the symbols in a slot are available for sidelink transmissions and the remaining symbols are reserved or used for the Uu transmissions for the shared band operation[39].

The points referred previously, like the frame and subframe, the slot it is schematized in the **Figure *19***,

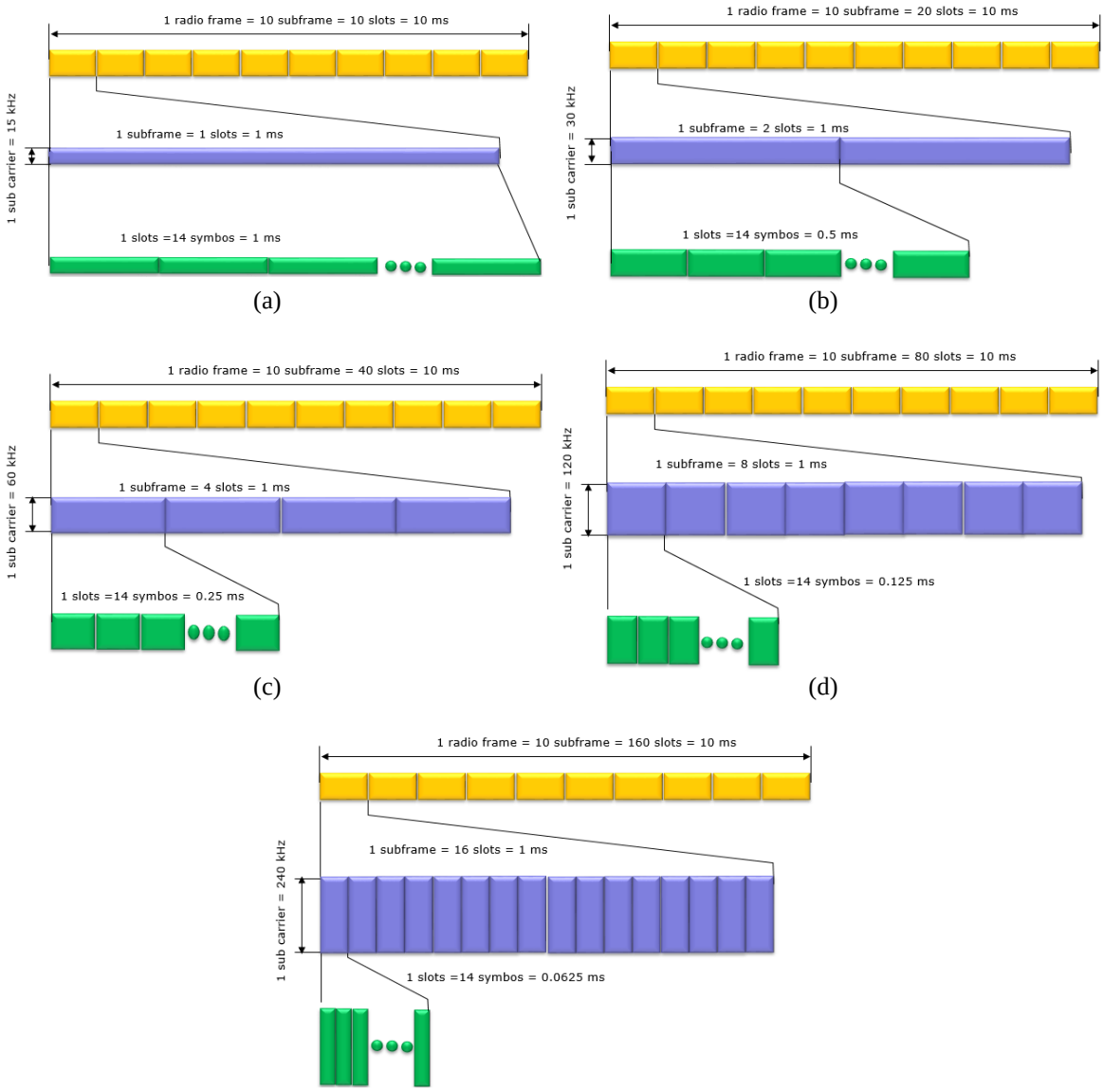

Figure 19. Resource Structure in the time domain (a) μ=0; (b) μ=1; (c) μ=2; (d) μ=3; (e) μ=4[35].

3.3.4 – Resource structure in the frequency domain

The resources in the frequency domain are formed by the following components, the resource element (RE) where each one RE is composed by a subcarrier over an OFDM symbol, also there is the resource block (RB) such RB it is composed from 12 consecutive subcarriers with the same Subcarrier Spacing (SCS). Also, one bandwidth of each RB depends on the SCS value of such subcarriers, where the resource grid it is composed of several RBs with the same SCS schematized on the **Figure *20***,

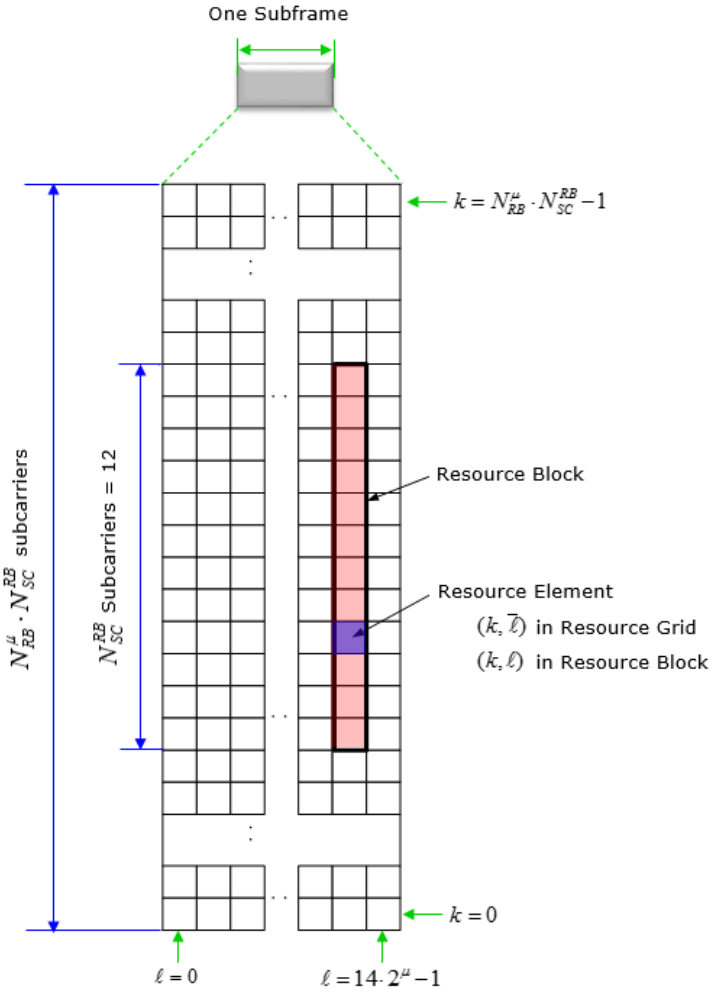

Figure 20. Resource Structure in the frequency domain [35].

The resources in the NR are organized in different Bandwidth Parts (BWP), which one of carriers may be up to 400 MHz, which is composed of 275 RBs, although, in most mobile services, a UE may not fully utilize these 275 RBs, and only a part of RBs may be used to confine the UE radio frequency, RF operation bandwidth for power saving. To cope with this situation, it is defined that the BWP it is composed with a set of following consecutive RBs within the carrier, for a UE, with a maximum number of BWPs that can be configured over a carrier, and at least one BWP can be activated at any time instant. At this concept elaborated before of the BWP, also leads with two types of RBs, the common RB, CRB, and physical RB, PRB, for a carrier composed with several RBs with the same numerology, these RBs are indexed increasingly from the lowest frequency of this carrier, in general, these RBs are called CRBs. Nevertheless, RBs that are included in a BWP are called as PRBs, and the indices of these RBs are reset and re-indexed increasingly. Finally for NR sidelink transmissions, at least one sidelink BWP can be configured on a carrier, and the minimum unit for resource scheduling in the frequency domain is a subchannel, which is composed of 10, 15, 20, 25, 50, 75, or 100 consecutive RBs depending on practical configuration [39].

3.4 – Physical channels and reference signals

At the NR sidelink there is the providing for the following physical channels and reference signals, schematized in the **Figure *21***,

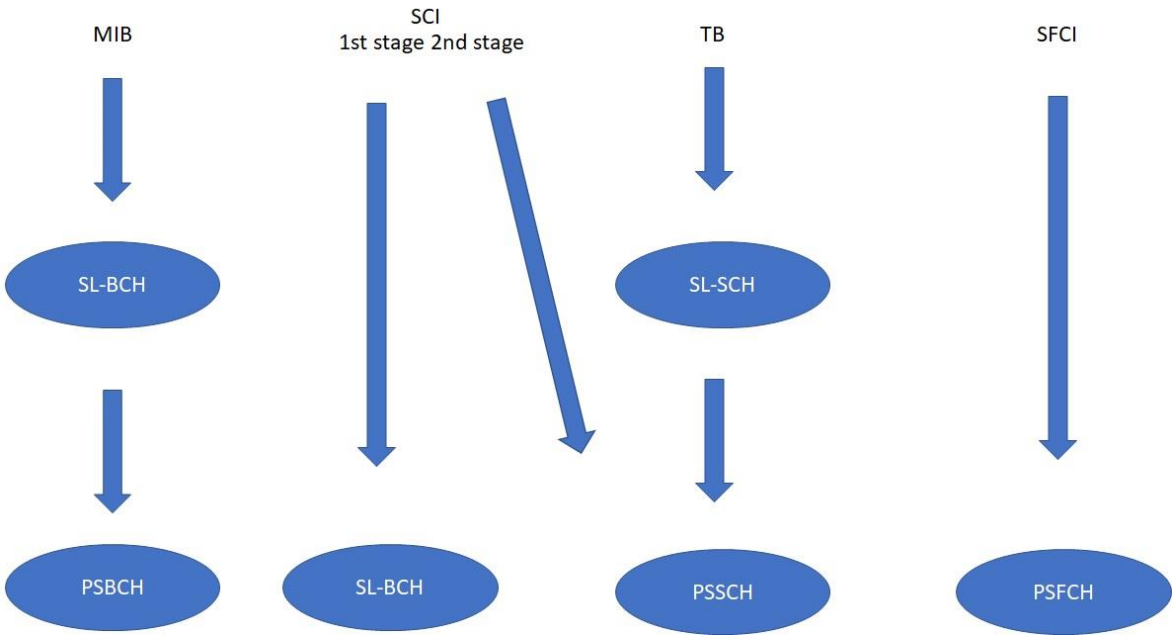

Figure 21. Physical channels and reference signal.

3.4.1 – Physical sidelink broadcast channel

The Physical Sidelink Broadcast Channel (PSBCH) is transmitted along with the Sidelink Primary Synchronization Signal and Sidelink Secondary Synchronization Signal (SPSS/SSSS) as we can see in the **Figure *22***. The Synchronization Signal Block (SSB) has the same numerology as PSCCH/PSSCH on that carrier, and an SSB should be transmitted within the bandwidth of the configured BWP. The PSBCH carries the MIB, which block will be detailed further. Finally, the SSB is transmitted periodically at every 160 ms, with the addition that, there are N repetitions within the 160 ms period with configurable starting offset and the interval, pre-configured depending on the SCS [39].

Figure 22. SSB schematic [36].

3.4.2 – Physical sidelink control channel

When the traffic to be sent to a receiving UE arrives at a transmitting UE, a transmitting UE should first send the PSCCH, which conveys a part of SCI to be decoded by any UE for the channel sensing purpose, including the reserved time-frequency resources for transmissions, demodulation reference signal (DMRS) pattern and antenna port, between others. For the PSCCH, the SCI is transmitted using quadrature phase shift keying (QPSK) with polar code[13].

3.4.3 – Physical sidelink shared channel

The PSSCH it is transmitted by a sidelink transmitting UE, which conveys for example sidelink transmission data, system information block (SIB) for RRC configuration, and a part of SCI. For the PSSCH, 16 QAM and 64 QAM with low density parity check (LDPC), code is supported, and 256 QAM can be possibly applied depending on the UE capability.[8].

As aforementioned, another part of SCI carries the remaining scheduling and control information to be decoded by the target receiving UE. It shares the associated PSSCH resources and the PSSCH DMRS with indications in the 1st-stage SCI for its resource allocation, and such a two-stage SCI design[13]

3.4.4 – Physical sidelink feedback channel

The physical sidelink feedback channel (PSFCH) is transmitted by a sidelink receiving UE for unicast and groupcast, which transmits one bit information over one RB for the HARQ ACK and for the negative ACK, NACK. In addition, channel state information (CSI) is carried in the MAC and control element (CE) over the PSSCH instead of the PSFCH[8].

3.4.5 – Reference signals

At the reference signals there is the Demodulation Reference Signal (DMRS), phase tracking reference signal (PT-RS) and channel state information reference signal (CSI-RS). These physical reference signals are supported by NR downlink/uplink transmissions and are also adopted by sidelink transmissions however the PT-RS is only applicable for FR2 transmission [37].

3.5 – Resource allocation

The NR sidelink transmissions have the following two modes of resource allocations, the mode 1, which the Sidelink resources are scheduled by a gNB, where the in-coverage UE is adopted. The mode 2, where the UE autonomously selects sidelink resources from a pre-configured sidelink resource pools based on the channel sensing mechanism and the in-coverage UE is adopted the out-of-coverage mode as well [13].

These resources are mapped in time and frequency domains as we can see in **Figure *23***. The smallest unit is the resource element (subcarrier *k*, symbol *l*), where $N_{RB,SC}^{SL} = 12$ subcarriers are a resource block (RB), with a subcarrier spacing equal to $15 \times 2^{\mu}$ kHz, and 14 OFDM symbols. Corresponding to a time slot, t_i^{SL}, as presented in 3.8, with $0 \le t_i^{SL} < 10240 \times 2^{\mu}, 0 \le i < T_{\max}$, where $\mu \in \{0,1,2,3,4\}$ defines the 5G-NR numerology [41].

In time domain, a set of 2^{μ} slots correspond to 1 ms, where it is exemplified in the table 2 the calculation of the subcarrier spacing and slot length. In frequency domain, we have N_{subCh}^{SL} subchannels with $N_{subChSize}^{SL}$ RBs each one, in a total of $N_{RB}^{SL} = N_{subCh}^{SL} N_{subChSize}^{SL}$ RBs available for sidelink transmissions.

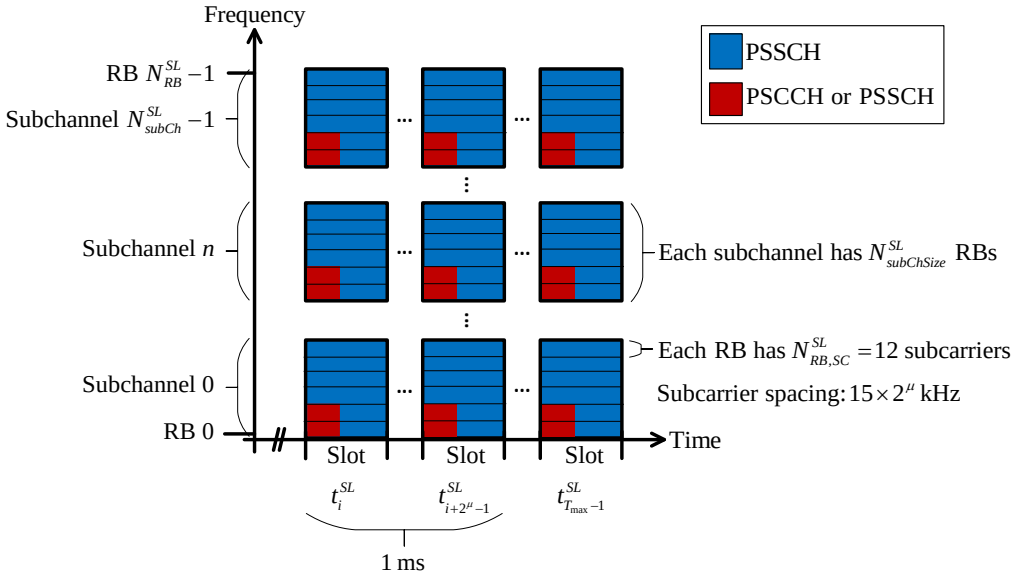

Figure 23. Resource Grid [38].

The PSCCH is allocated with the corresponding PSSCH in the same slot. The allocation of PSCCH starts in the second OFDM symbol of the time slot and it can have a duration of $T_{PSCCH} \in \{2,3\}$ symbols, which are pre-configured. In frequency domain, the PSCCH starts in the lowest RB of a subchannel, and it can occupy $N_{PSCCH} \in \{10,12,15,20,25\}$ RBs, where $N_{PSCCH} \le N_{subChSize}^{SL}$ is also a pre-configured value[42].

3.6 – Transport blocks

This topic has the purpose of referred the Master Information Block (MIB), what are its main characteristics and how its message is composed and transmitted. Further the objective is defining the Sidelink Information Control (SCI), the parameters of it message and how it is transmitted.

Finally, the transport block, its characteristics how to obtain the size of it, first knowing the type of codification, for example QPSK, 16QAM, between others, that it is in the SCI.

3.6.1 – Master information block

The Sidelink MIB(SL-MIB) it is carried on the Sidelink Broadcast Channel (SL-BCH) transmitted by the PSBCH. When this transmission occurs, the PSBCH transmits the MIB-V2X every 160 ms in the central 72 subcarriers of the Sidelink (SL) bandwidth.

The MIB message it is defined in **Table *3***,

Table 3. Master Information Block Message[43]

TDD-Config (12 bits)	In Coverage (1 bit)	Direct Frame Number (10 bits)	Slot Index (7 bits)	Reserved (2 bits)

- The TDD-Config which is assumed by the device transmitting the SL-MIB.
- In coverage parameter the value TRUE indicates that the UE transmitting the MasterInformationBlockSidelink is in network coverage.
- The direct frame number defines the frame number in which Sl-BCH transmitted.
- The Slot Index indicates the slot index in which S-SSB transmitted [43].

3.6.2 – Sidelink control information

The Sidelink Control (SCI) format 1-A, which it is carried by the PSCCH, with the following information and the bit occupation of which parameter in **Table *3***:

Table 4. SCI format 1-A [40].

Priority (3 bits)	Frequency resource assignment (10 or 11)	Time resource assignment (5 to 9 bits)	Resource reservation period	DMRS pattern	2nd-stage SCI format (2 bits)	Beta offset indicator (2 bits)	Number of DMRS (1 bit)	Modulation and coding scheme (5 bits)	Additional MCS table indicator (1 or 2 bits otherwise 0 bits)	PSFCH overhead indicator (2 or 4 bits otherwise 0 bits)	Reserved (0)

Therefore, the PSSCH allocation is indicated by the SCI through the frequency resource assignment and time resource assignment fields, in a form of time RIV (TRIV) and frequency RIV (FRIV), respectively, computed above and the starting subchannel of the first resource is $n_{start,0}$, which are obtained from FRIV.

The TRIV it is computed as in the next **algorithm *1***

algorithm 1: TRIV calculation [41]

1 $if\ N = 1$
2 $\quad TRIV = 0$
3 $elseif\ N = 2$
4 $\quad TRIV = t_1$
5 $else$
6 $\quad if\ (t_2 - t_1 - 1) \leq 15$
7 $\quad\quad TRIV = 30(t_2 - t_1 - 1) + t_1 + 31$
8 $\quad else$
9 $\quad\quad TRIV = 30(31 - t_2 - t_1) + 62 + t_1$
10 $\quad$ End
11 End

In the **algorithm *1***, where the value N indicates the location of the first resource in the slot where SCI format 1-A received and set the value of TRIV is set to 0 (line 2). Further that, the TRIV is settled to the value from the first resource time offset, t_1 (line 4). Finally will be compared the first and second, excluding the zero, resource time offset with the value of 15, computing the value of TRIV(line 7 and 9) [41].

The FRIV it is computed in the next algorithm *2*, which it is obtained following 2 conditions (line 1 and 3) ,firstly the starting sub-channel of the first resource , $n_{subch,0}^{start}$, determines the number as well of contiguously subchannels occupied by a PSCCH transmission , N_{PSSCH} . The number of alongside allocated sub-channels for each of the N resources, L_{subch} as well the starting sub-channel indexes of resources indicated by the received SCI format 1-A, except the resource in the slot where SCI format 1-A was received,

algorithm 2 FRIV calculation [41].

1 $if\ sl_{MaxNumberPerReserve} = 2$
2 $\quad FRIV = n_{subch,0}^{start} + \sum_{i=0}^{L_{subch}-1}(N_{subchannel}^{SL} + 1 - i)$
3 $if\ \ sl_{MaxNumberPerReserve} = 3$
4 $\quad FRIV = n_{subch,1}^{start} + n_{subch,2}^{start}\left(N_{subch}^{SL} + 1 - L_{subch}\right) + \sum_{i=0}^{L_{subch}-1}\left(N_{subchannel}^{SL} + 1 - i\right)^2$
5 End

Were,

- $n_{subch,1}^{start}$ represents the starting sub-channel index for the second resource
- $n_{subch,1}^{start}$represents the starting sub-channel index for the second resource
- $n_{subch,1}^{start}$ is the number of sub-channels in a resource pool provided according to the higher layer parameter slNumSubChannel [41].

3.6.3 – Transport block

As shown above, the SCI format 1-A contains the modulation and coding scheme, I_{MCS}. In order to compute the transport block size (TBS), when no additional MCS table is configured, it is used the **Table *5***[41].

Table 5. MCS index table 1 for PDSCH [34].

MCS Index I_{MCS}	Modulation Order Q_m	Target code Rate R x [1024]	Spectral efficiency
0	2	120	0.2344
1	2	193	0.3770
2	2	308	0.6016
3	2	449	0.8770
4	2	602	1.1758
5	4	378	1.4766
6	4	434	1.6953
7	4	490	1.9141
8	4	553	2.1602
9	4	616	2.4063
10	4	658	2.5703
11	6	466	2.7305
12	6	517	3.0293
13	6	567	3.3223
14	6	616	3.6094
15	6	666	3.9023
16	6	719	4.2129
17	6	772	4.5234
18	6	822	4.8164
19	6	873	5.1152
20	8	682.5	5.3320
21	8	711	5.5547
22	8	754	5.8906
23	8	797	6.2266
24	8	841	6.5703
25	8	885	6.9141
26	8	916.5	7.1602
27	8	948	7.4063
28	2	reserved	
29	4	reserved	
30	6	reserved	
31	8	reserved	

From **Table *5*** and I_{MCS}, the UE can determine the modulation order (Q_M), and target code rate (R) used in the PSSCH. Then the UE needs to determine the number of REs within the slot. The number of slots is given by,

$$N'_{RE} = N_{SC}^{RB} * (N_{symb}^{Sh} - N_{symb}^{PSFCH}) - N_{oh}^{PRB} - N_{RE}^{DMRS} \quad (1)$$

where:

- $N_{SC}^{RB} = 12$ is the number of subcarriers in a physical resource block.
- $N_{SC}^{RB} = sl\text{-}length\text{-}SLS\text{-}symbols\text{-}2$ where sl-lengthSLsymbols is the number of sidelink symbols within the slot provided by higher layer.

- $N_{Symb}^{PSFCH} = 3$ if "PSCH overhead indication" field of SCI format 1-A indicates "1", and $N_{Symb}^{PSFCH} = 0$ otherwise, if higher layer parameter $sl\text{-}PSFCH\text{-}Period$ is 2 or 4. If higher layer parameter $sl\text{-}PSFCH\text{-}Period$ is 1, $N_{Symb}^{PSFCH} = 3$.
- N_{oh}^{PRB} is the overhead given by higher layer parameter $sl - xOverhead$.
- N_{RE}^{DMRS} is given by the following table **Table *6***, according to the higher parameter $sl\text{-}PSFCH\text{-}Period$ [41].

Table 6. calculation of N_{RE}^{DMRS} [41]

sl-PSSCH-DMRS-TimePattern	N_{RE}^{DMRS}
{2}	12
{3}	18
{4}	24
{2,3}	15
{2,4}	18
{3,4}	21
{2,3,4}	18

$$N_{RE} = N'_{RE} * \eta_{PRB} - N_{RE}^{SCI,1} - N_{RE}^{SCI,2} \quad (2)$$

where:

- η_{PRB} is the total of allocated PRBs for the PSSCH.
- $N_{RE}^{SCI,1}$ is the total number of Res occupied by the PSSCH and PSCCH DMRS.
- $N_{RE}^{SCI,2}$ is the number of coded modulation symbols generated for the 2nd -stage SCI transmission [41].

Unquantized intermediate variable (N_{info}) is obtained by the following equation,

$$N_{info} = N_{RE} * R - Q_M - v \quad (3)$$

When $N_{info} \leq 3824$, the TBS is given by closest TBS of **Table *7*** that is not less than N'_{info} given by,

$$\mathrm{N'_{info}} = \max\ 24, 2^{\mathrm{n}} * (\frac{\mathrm{N_{info}}}{2^n}) \quad (4)$$

Were,

$\mathrm{n} = \max(3, [\log_2(n_{info}) - 6]$ [41].

Table 7. TBS for N_info≤3824 [34]

Index	TBS	Index	TBS	Index	TBS	Index	TBS
1	24	31	336	61	1288	91	3624
2	32	32	352	62	1320	92	3752
3	40	33	368	63	1352	93	3824
4	48	34	384	64	1416		
5	56	35	408	65	1480		
6	64	36	432	66	1544		
7	72	37	456	67	1608		
8	80	38	480	68	1672		
9	88	39	504	69	1736		
10	96	40	528	70	1800		
11	104	41	552	71	1864		
12	112	42	576	72	1928		
13	120	43	608	73	2024		
14	128	44	640	74	2088		
15	136	45	672	75	2152		
16	144	46	704	76	2216		
17	152	47	736	77	2280		
18	160	48	768	78	2408		
19	168	49	808	79	2472		
20	176	50	848	80	2536		
21	184	51	888	81	2600		
22	192	52	928	82	2664		
23	208	53	984	83	2728		
24	224	54	1032	84	2792		
25	240	55	1064	85	2856		
26	256	56	1128	86	2976		
27	272	57	1160	87	3104		
28	288	58	1192	88	3240		
29	304	59	1224	89	3368		
30	320	60	1256	90	3496		

3.7 – Main differences between LTE-V2X and NR-V2X

The main differences between LTE-V2X and NR-V2X are based in the specification, where in the LTE-V2X it is the 3GPP between the Release-14 to Release-15 and in NR-V2X it is 3GPP between the Release-16 to Release-17, in terms of latency the LTE-V2X has a low latency, in order of 10 to 100 milliseconds and the NR-V2X has a ultra-low latency in the range of an 1 millisecond. In terms of PC5 interface message type, the LTE-V2X just use a Broadcast type of message but NR-V2X uses Broadcast, Unicast and the Groupcast type of messages and the application scenarios from the LTE-V2X it is based in safety related and the NR-V2X it is used in advanced applications. In terms of cellular network coverage, the LTE-V2X use the PC5 Mode 3 and the NR-V2X uses the PC5 Mode 2, which both correspond the fact of the transmission resources of the PSCCH and from the PSSCH are indicated by the eNB in and out of cellular network coverage, LTE-V2X uses the

PC5 mode 4 and the NR-V2X uses the PC5 mode 2, which them correspond the curiosity that the same resources are not indicated by the eNB,

Table 8. main differences between LTE-V2X and NR-V2X [37]

Items	**LTE-V2X**	**NR-V2X**
Specification	3GPP Rel-14/Rel-15	3GPP Rel-16/Rel-17
Latency	Low Latency: 10 ~ 100 ms	Ultra-low latency: 1ms
PC5 Message Type	Broadcast	Broadcast, Unicast and Groupcast
Application Scenario	Safety related/Enhaced	Advanced Application
Cellular Network Coverage	Uu and PC5 mode3	Uu and PC5 Mode1
Out of Cellular Network Coverage	Pc5 Mode 4	PC5 Mode 2

Besides these main differences, there are some others to take in consideration like,

- Each subframe has two slots available, in LTE-V2X however in NR-V2X, the number of subframes depends on the spacing of carrier, so if we have 15 kHz, we have like one slot per subframe and if we have 240 kHz, we have 16 slots per subframe, increasing the number of slots in an exponential way.
- The number of symbols per each slot, in LTE-V2X, it is fixed with 6 or 7 symbols but in NR-V2X it is also fixed with 14 symbols, which one can be split into mini-slots of 2,4 or 7 symbols.
- In terms of channels, we have logical, transport and physical channels, in both technologies, although in LTE-V2X we use the Cell Specified Signal (CRS) where one cell specific reference signal is transmitted from each downlink antenna port. This downlink cell specific reference signal can be used for cell search and initial acquisition, downlink channel quality measurements and downlink channel estimation for coherent demodulation and detection at the UE, to a different channel mapping where is used the PT-RS. Where the PHICH and PCCICH have been remove, the HARQ operation has also been updated to be more flexible and the PDCCH is now administered by layer 3 procedures.

- Finally, the channel is coded, in the LTE-V2X with turbo code in terms of data, which is are a class of high-performance forward error correction, FEC, with an perform well due to the attractive combination of the code's random appearance on the channel together with the physically realisable decoding structure, and so this codes are affected by an error floor and for control the Tail-Biting Convolutional Code, TBCC, s used for encoding downlink and uplink control channels, terminating the trellis of a convolutional code is a key parameter in the code's performance for packet-based communications. In the NR-V2X the data it is coded by low-density parity-check, LDPC, this code is a linear error correcting code, a method of transmitting a message over a noisy transmission channel, compared with the turbo code on LTE-V2X, the BER performance of Turbo codes is influenced by low codes limitations, however LDPC codes have no limitations of minimum distance, that indirectly means that LDPC codes may be more efficient on relatively large code rates than Turbo codes. But LDPC codes are not the complete replacement, turbo codes are the best solution at the lower code rates. And the control is coded by a polar code is a linear block error-correcting code, this code construction is based on a multiple recursive concatenation of a short kernel code which transforms the physical channel into virtual outer channels, also there is a schematic of the synchronization subframe of both technologies[44].

Chapter 4 – Proposed algorithm for effective PSCCH searching

Cooperative Intelligent Transport Systems (C-ITS) are essential for increasing the road safety and to make road transport more efficient, sustainable, and environmentally friendly. The implementation of C-ITS technology is only possible through connectivity Vehicle-to-Everything (V2X), which allows the interconnection of vehicles in a network and with road a support infrastructure. However, real-time systems require efficient signal processing in order to respond within the necessary time. Some of this processing is related to searching the Physical Sidelink Control Channel (PSCCH), where a blind algorithm is commonly used. However, this algorithm is quite inefficient to searching the PSCCH, since all the processing should be done several times before successful decoding it. Therefore, through this chapter it is presented the design of a more efficient algorithm to search/decode the PSCCH. In the proposed algorithm, we firstly compute all the correlations between the received signal and the Demodulation Reference Signal (DMRS), and the remaining conventional processing to decode the PSCCH is only performed over the subchannels with higher correlation, which leads to a strong complexity reduction. The proposed algorithm is evaluated and compared with the conventional blind algorithm. The results have shown a significant performance improvement in terms of runtime.

4.1 – State of art

In this section we present the state-of-art regarding the main topic of this dissertation. In [13], an approach based on measure the reference signals received power (RSRP) was described. During the sensing window, the transmitting UE measures the RSRP of all subchannels, and if a subchannel does not exceed a threshold, this subchannel becomes a candidate. Moreover, a transmitting UE needs to detect the PSCCH transmitted by other UEs and get the SCI, to know which subchannels are occupied. For this purpose, it is not needed all the elds of SCI, so they are transmitted in two stages. The first stage of SCI is transmitted over PSCCH, while the second one is transmitted over PSSCH. The first stage SCI decoding is based on a blind detection. When the first stage SCI

decoding fails, the second stage SCI decoding also fails. After the sensing window, we have the selection window, where the candidate subchannels are selected and occupied. In , an open-source, fullstack, end-to-end, standard-compliant network simulator was presented, where the physical layer receives the first stage SCI transmitted over PSCCH to measure the RSRP and to get the information about the possible PSSCH. The RSRP is computed using the 3 resource elements per RB, carrying the first stage SCI, because the simulator does not explicitly have PSCCH DMRS. In [45], the authors proposed an enhancement to the sensing-based semi-persistent scheduling to reflect the stochastic nature of the aperiodic traffic on the resource allocation, to reduce the packet collisions. The authors of [46], proposed a method for pedestrian UEs that operates with partial sensing, which is used to reduce the power consumption, in order to enhancing the throughput. For this, an additional UE, i.e., an RSU, is used to collect the sensing results from each UE. Then, the RSU aligns all of the partial sensing windows to provide a more efficient sensing result.

In [47], the collision probability via the random selection of resources was analyzed, and the deep reinforcement learning algorithm was investigated, which decreases the collision probability by using a platoon leader to learn from the communication environment. In [48] , a group scheduling mechanism is proposed, where a platoon leader takes charge of the whole platoon. It is platoon leader which granted the resources by the network and distributes the scheduling information by the remaining platoon.

The authors of[49], to address the latency problem, proposed the hyper-fraction channel allocation method, where the road is divided into several zones and for each zone, a channel is allocated. Then, when a UE is located within a certain zone, this one uses the channel allocated to the zone. In [50], a cluster-based resource selection scheme is proposed to reduce the resource collision. In this scheme, the resources are divided into different resource sets, then each cluster head selects its resource set based on measurement. The authors of [51], proposed a clustering-based resource management scheme for latency and sum rate optimization. First, it is performed an optimization of the total average sum rate of each link, and then cluster based optimum algorithms are proposed to get the optimum resource management.

In [52], a method to minimize the interference between UEs was proposed. For that, an optimization problem is expressed as a mixed binary integer nonlinear programming, subject to the quality of service, the total available power, the interference threshold, and the minimal transmission rate. The authors of [53], proposed a vehicle density based two-stage resource management scheme to reduce latency, improve throughput and reliability for V2V and V2N. In the first stage, the density information for the resource distribution strategy is explored, then, in the second stage, the channel state information and queuing state information are used [54].

4.2 – System model

In this dissertation we consider a 5G-NR V2X sidelink system, which uses the Cyclic Prefix Orthogonal Frequency Division Multiplexing (CP-OFDM) as the access technique. For the sake of simplicity and, without loss of generality, we consider only 2 UEs, where the transmitter and receiver UE are equipped with N_{tx} and N_{rx} antennas, respectively. The UEs are communicating based on a resource allocation scheme defined in mode 2, **Figure *24***, in other words, both UEs are out of coverage and have autonomous resource selection.

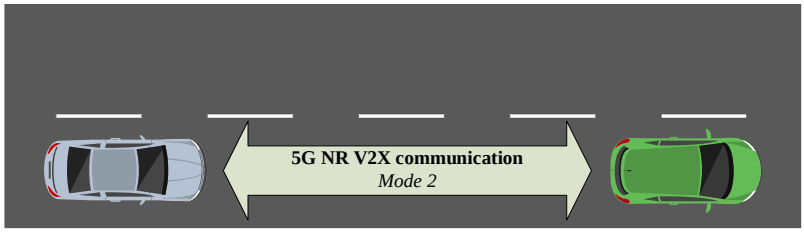

Figure 24. System Model [54]

The DMRS associated to PSCCH for subcarrier k and symbol l within the slot, $d^{i}_{PSCCH,k,l}$, used in channel estimation are given by [55]

$$d^{i}_{PSCCH,k,l} = \beta_{PSCCH} w_i(k') r_l(3m+k'), \qquad (5)$$

Where $k = mN^{SL}_{RB,SC} + 4k' + 1$, $k' = 0,1,2$ and $m = 0,1,\ldots$. The amplitude scaling factor β_{PSCCH} is applied to transmit with the power specified in [56] , and the quantity $w_i(k')$ is given by , where $i \in \{0,1,2\}$ shall be randomly selected [55]

Table 9. The quantity $w_i(k')$ [54]

		i		
		0	1	2
k'	0	1	1	1
	1	1	$e^{j\frac{2}{3}\pi}$	$e^{-j\frac{2}{3}\pi}$
	2	1	$e^{-j\frac{2}{3}\pi}$	$e^{j\frac{2}{3}\pi}$

Finally, $r_l(u)$, $u = 0,1,\ldots$ is a sequence generated by

$$r_l(u) = \frac{1}{\sqrt{2}}\left(1 - 2c\left(2u\right)\right) + j\frac{1}{\sqrt{2}}\left(1 - 2c\left(2u+1\right)\right), \quad (6)$$

where $c(u)$ is a pseudo-random sequence defined in [55].

Let be $s_q \in \mathrm{C}$, with $q = 0,1,\ldots$, the OFDM waveform samples which carry the PSCCH/PSSCH resources allocated as in Figure 3-10, and the synchronization signal blocks. The transmitted signal, $\mathbf{s}_{tx,q} \in \mathrm{C}^{N_{tx}}$, is given by

$$\mathbf{s}_{tx,q} = \mathbf{f}_a s_q, \quad (7)$$

where $\mathbf{f}_a \in \mathrm{C}^{N_{tx}}$ is the precoder. Since our focus is only on the PSCCH search algorithm, we consider the simple random precoder discussed in [57], and given by

$$\mathbf{f}_a = [\mathrm{e}^{j2\pi\omega_v}]_{1\le v\le N_{tx}}, \quad (8)$$

where ω_v, $v \in \{1,\ldots,N_{tx}\}$ are i.i.d. uniform random variables with support $\omega_v \in [0,1]$. At receiver side, a minimum mean-squared error (MMSE) equalizer is adopted and applied to received signal $\mathbf{s}_{rx,q} \in \mathrm{C}^{N_{rx}}$, $q = 0,1,\ldots$, where the channel between the transmitter and receiver is estimated based on DMRS [54].

4.3 – Receiver design

This topic presents the proposed algorithm for the received signal processing. Firstly, the general receiver processing is introduced, and then, the commonly used blind algorithm is discussed. After that, a brief study on the correlation of the received signal with the DMRS is presented. Based on this study, a new algorithm is proposed and finally a theoretical runtime analysis is performed [54].

4.3.1 – Receiver model

The block diagram of the received signal processing is shown in **Figure *25***. It has three parts: 1) synchronization procedures; 2) get control information; and 3) get the desired data.

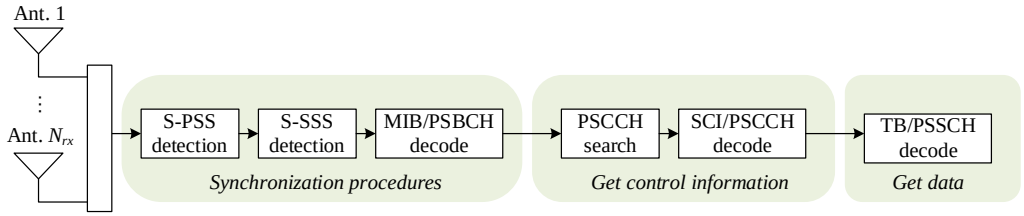

Figure 25. Block diagram of the receiver [47].

The first step of the receiver is to try to synchronize with the transmitter. For that, the receiver knows the possible Sidelink Primary Synchronization Signals (S-PSS) and performs a correlation with the received signal until it finds a significant peak. After finding the S-PSS, the receiver also performs a correlation between known sequences of the S-SSS and the received signal. Considering the S-PSS/S-SSS sequences that gave the main correlation peaks, a sidelink identity is obtained, which is then used to try to decode the MIB. If the MIB is successfully decoded, then the receiver proceeds to the next step. Otherwise, the receiver goes back to the beginning and continues trying to synchronize.

Once the MIB is obtained, the receiver is ready to search for PSCCHs. As mentioned above, the resource grid is organized into subchannels, and the PSCCH starts in the lowest RB of a subchannel. Moreover, the DMRS associated to PSCCH are computed based on the quantity $w_i\left(k'\right)$, where $i \in \left\{0,1,2\right\}$ shall be randomly selected. Therefore, the receiver needs to search for PSCCHs in different subchannels and needs to try different indexes i until decode the SCI/PSCCH. Thus, only after this, it is possible to get the SCI carried in the PSCCH and extract the desired data, i.e., TB from the PSSCH.

To proceed with the PSCCH search, an algorithm is needed. The most used is the blind algorithm [13], whose pseudo-code is presented in

algorithm 3: Blind Algorithm [54].

1	For $n = 0,...,N_{subCh}^{SL} - 1$ do
2	For $i = 1,2,3$ do
3	$\mathbf{c}_{n,i} = \sum_{v=1}^{N_{rx}} \text{corr}(\mathbf{s}_{rx,v}, \mathbf{d}_{PSCCH}^{n,i})$
4	Compute $f_{offset}(q_{\max})$, where $q_{\max} = \arg \max_{q \in \{0,...,Q_{\max}-1\}} \mathbf{c}_{n,i}(q)$
5	$\mathbf{s}_{rx,v}^{sync}(q) = \mathbf{s}_{rx,v}(q + f_{offset}),\ q = 0,...,Q_{\max} - 1 - f_{offset}$
6	Perform the CP-OFDM demodulation
7	Extract the PSCCH candidate
8	Perform the PSCCH channel estimation
9	Perform the MMSE equalization
10	Try to decode the PSCCH
11	Try to decode the SCI
12	If SCI decoded with success then
13	Break
14	End
15	End
16	End

As we can see in **algorithm *3***, we search in all subchannels (line 1), for all indexes i (line 2) until decode the SCI/PSCCH (lines 12-14). In the PSCCH decoding processing, first we compute the correlation of received signal by each antenna, $\mathbf{s}_{rx,v} = \left[s_{rx,v}(0),...,s_{rx,v}(Q_{\max} - 1) \right]^T$, $v = 1,...N_{rx}$, where $Q_{\max}$ is the maximum number of samples used in the correlation, with the DMRS, $\mathbf{d}_{PSCCH}^{n,i} = \left[..., d_{PSCCH,k,l}^{i}, ... \right]^T$, $k = nN_{subChSize}^{SL} N_{RB,SC}^{SL} + 4k' + 1$, $k' = 0,1,2$, $l = 1,...,T_{PSCCH}$ (line 3). Then, the frame offset, $f_{offset}(q_{\max})$, is computed using the index number of sample where the correlation peak is stronger (line 4) and a subframe synchronization is done (line 5). After that, the CP-OFDM demodulation is performed (line 6), the PSCCH candidate for subchannel n is extracted (line 7), the channel estimation using $\mathbf{d}_{PSCCH}^{n,i}$ is performed (line 8), and then the MMSE equalization is done using the estimated channel (line 9). Finally, we try to decode the PSCCH and SCI (lines 10-11) [54].

4.3.2 – Correlation analysis

An analysis of the correlations performed in **algorithm *3***, line 3, is done in this Section. If the received signal has a PSCCH present in a subchannel n with DMRS using an index i, it would be expected to have a stronger correlation peak when $\text{corr}(\mathbf{s}_{rx,v}, \mathbf{d}_{PSCCH}^{n,i})$ is done. We observed it by

transmitting a signal with a PSCCH on the subchannel $n=1$ and DMRS using the index $i=1$. This test is done for a scenario where the signal-to-noise-ratio (SNR) is set to $-10\,\text{dB}$. The remaining parameters are $N_{RB}^{SL}=50$, $N_{subChSize}^{SL}=10$, $N_{subCh}^{SL}=5$, $N_{PSCCH}=10$, $T_{PSCCH}=3$, $N_{PSSCH}=1$, $N_{tx}=16$ and $N_{rx}=16$. The results are shown in **Figure *26***.

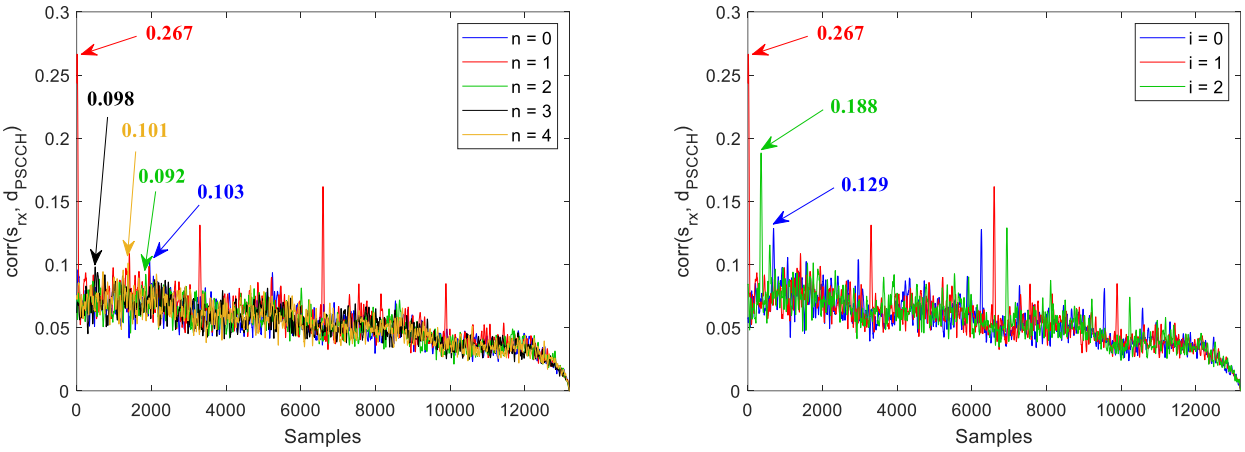

(**a**) (**b**)

Figure 26. Correlation results: (a) Trying different subchannels with i=1; (b) Trying in subchannel for indexes i=0, 1 and 2 [54].

As we can see in **Figure *26***(a), the peak associated to the right subchannel, 0.267, is much higher than the other peaks associated to other subchannels, 0.103, 0.101, 0.098 and 0.092. Thus, the use of this information can be very effective in determining the right subchannel. Moreover, we can also see in **Figure *26***(b),that the peak associated to the right index i is higher than the other peaks, although not as prominently as **Figure *26***(a). Therefore, we can also use this information in determining the right index i [54].

4.3.3 – Propose effective PSCCH searching based on correlation

Based on the observations of the previous Section, we now design a new efficient algorithm, where all correlations are firstly done, without performing all the remaining process. After that, the processing for SCI/PSCCH search and decoding are done for the pair (n,i), where the correlation is stronger and it continues in descending order. The pseudo-code of proposed algorithm is presented in **algorithm *4***.

algorithm 4: Proposed effective PSCCH searching based on correlation [54].

1 For $n = 0,...,N_{subCh}^{SL} - 1$ do
2 For $i = 1,2,3$ do
3 $\mathbf{c}_{n,i} = \sum_{v=1}^{N_{rx}} \text{corr}(\mathbf{s}_{rx,v}, \mathbf{d}_{PSCCH}^{n,i})$
4 $\mathbf{c}^{\max}(3n+i-1) = \max\left(\mathbf{c}_{n,i}\right)$
5 End
6 End
7 $(\mathbf{c}^{sorted}, \mathbf{c}_{indexes}^{sorted}) = \text{sort}_{desc}\left(\mathbf{c}^{\max}\right)$
8 For $p = 0,...,3N_{subCh}^{SL} - 1$ do
9 $n = \mathbf{c}_{indexes}^{sorted}(p) / 3$
10 $i = \text{rem}\left(\mathbf{c}_{indexes}^{sorted}(p), 3\right) - 1$
11 Compute $f_{offset}(q_{\max})$, where $q_{\max} = \arg \max_{q \in \{0,...,Q_{\max}-1\}} \mathbf{c}_{n,i}(q)$
12 $\mathbf{s}_{rx,v}^{sync}(q) = \mathbf{s}_{rx,v}(q + f_{offset}),\ q = 0,...,Q_{\max} - 1 - f_{offset}$
13 Perform the CP-OFDM demodulation
14 Extract the PSCCH candidate
15 Perform the PSCCH channel estimation
16 Perform the MMSE equalization
17 Try to decode the PSCCH
18 Try to decode the SCI
19 If SCI decoded with success then
20 Break
21 End
22 End

In **algorithm *3***, first we compute for all subchannels (line 1) and all indexes i (line 2), the correlations $\text{corr}(\mathbf{s}_{rx,v}, \mathbf{d}_{PSCCH}^{n,i})$ (line 3), and store the value of main peak associated to each pair (n,i) in $\mathbf{c}^{\max} \in \mathbb{R}^{3N_{subCh}^{SL}}$ (line 4). After that, we sort the vector $\mathbf{c}^{\max}$ in descending order and store the indexes of original positions in $\mathbf{c}_{indexes}^{sorted} \in \mathbb{R}^{3N_{subCh}^{SL}}$ (line 7). Then, for each element of $\mathbf{c}_{indexes}^{sorted}$, we get the pair (n,i) (lines 9-10), and we apply the remain processing (lines 11-21), similar to **algorithm *4***[54].

4.3.4 – Theorical runtime analysis

In this Section, a theoretical runtime analysis is done, to compare the performances of the two presented algorithms, i.e., the conventional **algorithm *3***, and the proposed **algorithm *4***. For that, first let's define the processing time of each part of the algorithms. These definitions are presented in **Table *10***.

Table 10. Runtime definitions [54].

Symbol	Designation	Rows of **algorithm *3***	Rows of **algorithm *4***
T_{corr}	Compute correlation	3	3
T_{fmax}	Find the maximum correlation	-	4
T_{sort}	Sort the maximum correlations	-	5
T_{gpair}	Get the pair (n,i)	-	6-7
T_{rem}	Remain processing	4-14	11-21

Let be E_1 and E_2 the expected number of attempts associated to **algorithm *3*** and **algorithm *4***, respectively. Therefore, the total runtime needed to perform the search and decoding procedure of an SCI/PSCCH, associated to **algorithm *3*** and **algorithm *4***, are respectively given by

$$T_1 = E_1\left(T_{corr} + T_{rem}\right), \tag{9}$$

$$T_2 = 3N_{subCh}^{SL}\left(T_{corr} + T_{fmax}\right) + T_{sort} + E_2\left(T_{gpair} + T_{rem}\right). \tag{10}$$

For a low SNR scenario, $E_1 = E_2 = 3N_{subCh}^{SL}$, and from (9) and (10) we obtain

$$T_1 = 3N_{subCh}^{SL}\left(T_{corr} + T_{rem}\right), \tag{11}$$

$$T_2 = 3N_{subCh}^{SL}\left(T_{corr} + T_{fmax} + T_{gpair} + T_{rem}\right) + T_{sort}. \tag{12}$$

Since T_{fmax}, T_{gpair} and T_{sort} are much lower than T_{corr} or T_{rem}, for a low SNR scenario, we conclude that $T_1 \approx T_2$.

For a high SNR scenario, $E_1 = \frac{1}{2}\left(3N_{subCh}^{SL} + 1\right)$ and $E_2 = 1$. Then, from (9) and (10) we obtain

$$T_1 = 1.5N_{subCh}^{SL}T_{corr} + 1.5N_{subCh}^{SL}T_{rem} + 0.5T_{corr} + 0.5T_{rem}, \tag{13}$$

$$T_2 = 3N_{subCh}^{SL}T_{corr} + T_{rem} + 3N_{subCh}^{SL}T_{fmax} + T_{sort} + T_{gpair}. \tag{14}$$

Since T_{fmax}, T_{gpair} and T_{sort} are much lower than T_{corr} or T_{rem}, then $T_2 \approx 3N_{subCh}^{SL}T_{corr} + T_{rem}$. Therefore, the **algorithm *4*** has a clear advantage over the **algorithm *3***when $T_2 < T_1 \Leftrightarrow T_{corr} < T_{rem}$, which is generally true, since T_{rem} includes CP-OFDM demodulation, PSCCH channel estimation, MMSE equalization and the SCI/PSCCH decoding[54].

4.4 – Performance results

In this section, we compare the performance of **algorithm *3*** (blind based) and **algorithm *4***(correlation based). For that, we assume a scenario where $N_{subChSize}^{SL}=10$, $N_{PSCCH}=10$, $T_{PSCCH}=3$, $N_{PSSCH}=1$, $N_{tx}=16$ and $N_{rx}=16$. The PSCCH is transmitted in a subchannel $n\in\{0,...,N_{subCh}^{SL}-1\}$ selected randomly and associated to DMRS with a random index $i\in\{0,1,2\}$. We tested with $N_{RB}^{SL}=50$ and $N_{RB}^{SL}=100$, therefore $N_{subCh}^{SL}=N_{RB}^{SL}/N_{subChSize}^{SL}$ is 5 or 10. Finally, the results were obtained on a machine with Intel(R) Core(TM) i7-10750H CPU @ 2.60GHz and 16.0 GB of RAM.

Figure *27* shows the comparision of the SCI BLER performance for **algorithm *3*** and **algorithm *4*** .For both cases, almost all blocks failed to decode until $\text{SNR}=-18\,\text{dB}$ and almost all blocks were successful when decoding above $\text{SNR}=-12\,\text{dB}$. So, there was a significant improvement going from -18 to -12 dB. Moreover, we can observe that the performance obtained for the two algorithms almost overlaps [54].

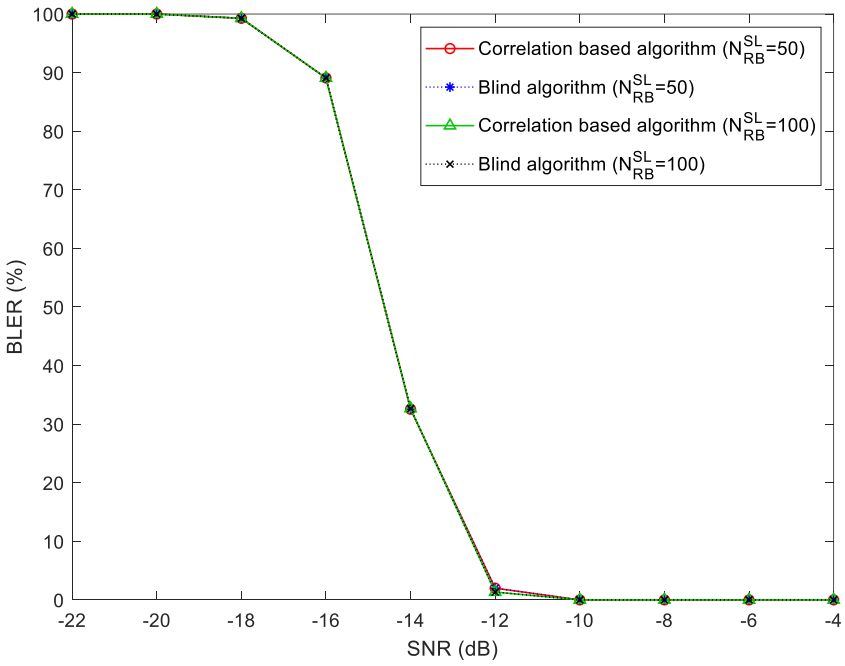

Figure 27. SCI BLER [54].

Figure *28* shows the throughput obtained for both algorithms. As we can see, the throughput is very low until $\text{SNR}=-12\,\text{dB}$ and it is almost 100% when above $\text{SNR}=-8\,\text{dB}$. Therefore, we also have a sudden performance improvement, although this only occurs for slightly higher SNR, when

comparing with the results in **Figure *27***. The throughput obtained for the two algorithms practically overlaps [54].

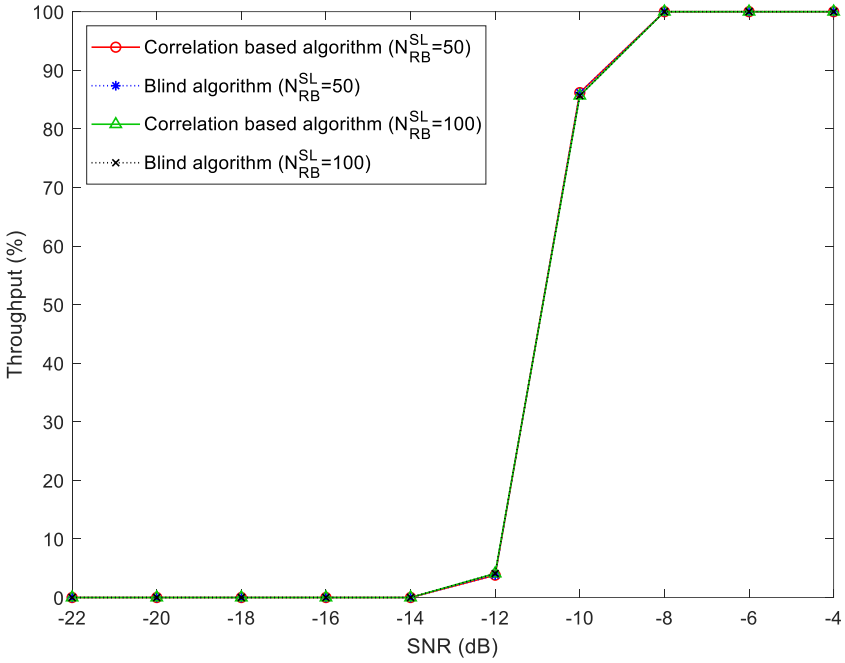

Figure 28. Throughput for PSSCH [54].

Figure *29* shows the average number of attempts for **algorithm *3*** and **algorithm *4***, for $N_{RB}^{SL}=50$ and $N_{RB}^{SL}=100$ ($N_{subCh}^{SL}=5$ and $N_{subCh}^{SL}=10$, respectively). As mentioned above, for low SNR, $E_1=E_2=3N_{subCh}^{SL}$. Then, for $N_{RB}^{SL}=50$ we have $E_1=E_2=15$, and for $N_{RB}^{SL}=100$ we have $E_1=E_2=30$, which is validated in Error! Reference source not found.. Moreover, for high SNR, EMBED Equation.DSMT4 $E_1=\frac{1}{2}\left(3N_{subCh}^{SL}+1\right)$ and $E_2=1$. Then, for $N_{RB}^{SL}=50$ we have $E_1=8$, and for $N_{RB}^{SL}=100$ we have $E_1=15.5$, which is also validated in **Figure *29***. As shown in **Figure *27*** and **Figure *28***, the same performance in terms of BLER and throughput was achieved, but with a much lower number of attempts to decode the PSCCH at it can be seen in **Figure *29***. Similar to **Figure *27***, almost all attempts failed until $\mathrm{SNR}=-18\,\mathrm{dB}$ and the best performance is achieved above $\mathrm{SNR}=-12\,\mathrm{dB}$ [54].

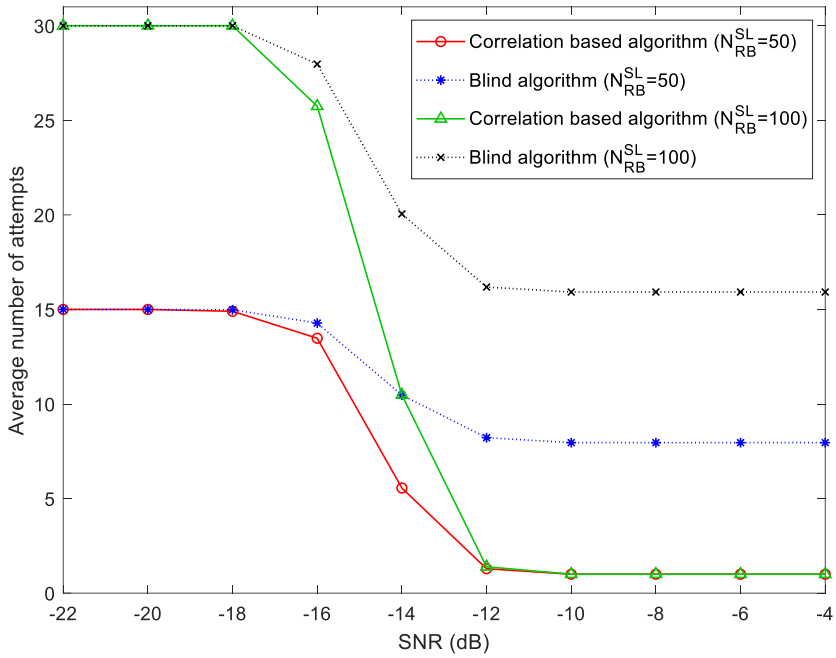

Figure 29. Average number of attempts [54].

Figure *30* shows the runtime measures for PSCCH search/decoding. As expected, the correlation based algorithm is better for high SNR regime, when compared with the correspondent blind algorithm result. In high SNR regime, we have for $N_{RB}^{SL}=50$, a total runtime $T_1=0.9\text{s}$ and $T_2=0.4\text{s}$, and for $N_{RB}^{SL}=100$, we have $T_1=3.0\text{s}$ and $T_2=1.6\text{s}$. Therefore, in both cases the runtime

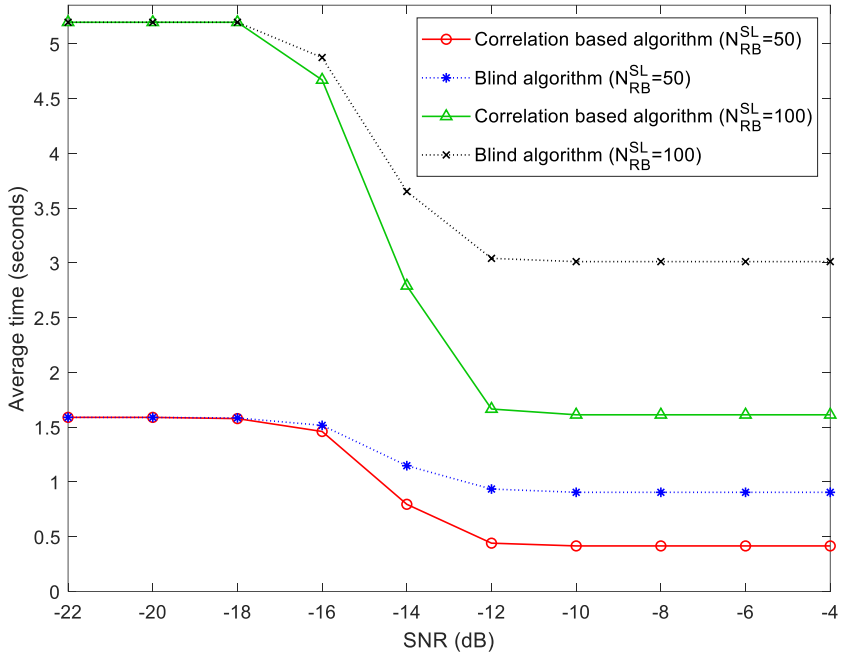

Figure 30. Average time for PSCCH search/decoding(seconds) [54].

Finally, **Figure *30*** shows the same results of **Figure *31***, but in a normalized way to the highest time, so that we can analyse the results, without these being associated with a specific CPU. In the high SNR zone, the gap for $N_{RB}^{SL}=50$ is 30.8%, while for $N_{RB}^{SL}=100$ is 26.9%. This means that the proposed correlation based algorithm, even though it continues to show a clear improvement over the blind algorithm, it lost some effectiveness by increasing the N_{RB}^{SL}. This is associated with the fact that the bandwidth is greater, and that more samples are being processed in calculating the correlations [54].

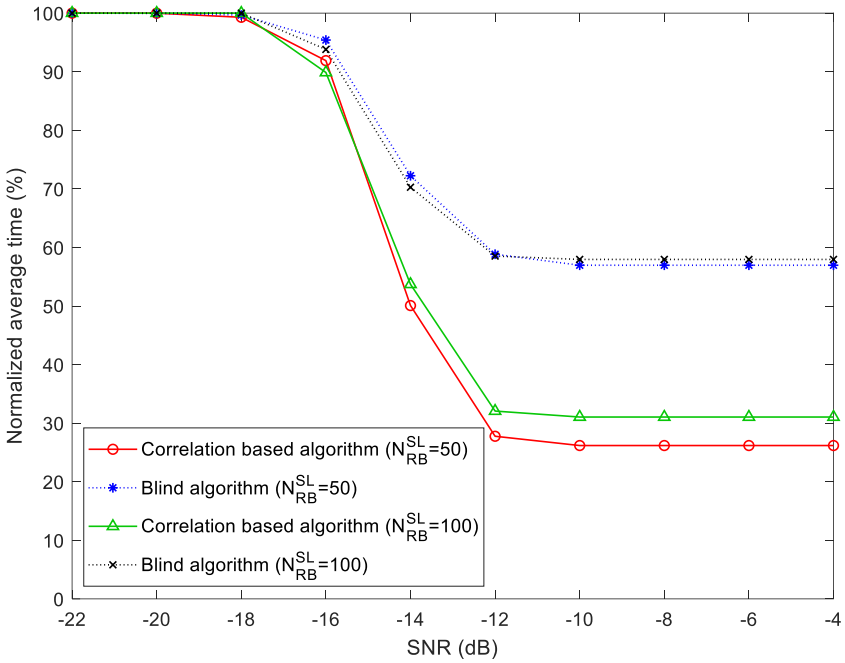

Figure 31. Normalized average time for PSCCH search/decoding (%) [54].

Chapter 5 – Conclusions and future work

In this last chapter we point out the main conclusions about the work developed in this dissertation, which can be really important in the society as we know, bringing other types of features like the communication between two vehicles, preventing accidents and permitting them being driven with each other and without a user, the of spoken platooning effect. The communications between the vehicle and the infrastructure, like for example the highway and it belonged signals, like speed control and bad weather advice. Also, the simple communication vehicle to pedestrian, that allows a vehicle to communicate with a person that is walking on the road, preventing a possible accident as well.

5.1 – Conclusions

This work is based in a research and test of 5G V2X radio communications to support the autonomous driving, which is analyse the existing algorithms in searching and trying to decode the PSCCH. Testing them in terms of performance and improve them in a way to become this search and decoding way faster that originally is. Firstly, in order to achieve this goal, was important to the understand the evolution of the mobile network, from the old one 1G to the newer and better 5G, as well the physical layer of this last one, where this work is focused on.

After understanding the evolution of the mobile network, it was important as well, figure out why the importance to evolve from the one generation to the next one. In this case what was the factors that force the evolution from 4G to 5G, like for example the need from the society using more devices, need faster access to the internet, and so on. For the need of this evolution, the emerging of new technologies, like mmWave, mMimo and small cells, was significant for the 5G success. For measure the reliability of this new mobile network was defined some indicators, like growth, the number of 5G connected devices, in terms of efficiency, for example the cost and energy efficiency and in matter of performance, in other words the connection density. This new mobile generation besides brings new needs, brings besides low latency and enhanced mobile broadband brings a new type of communications, the vehicular communications. Was studied the network architecture as well from the 5G, how it networks core was divided in two, like the user and control, and

understanding the constitution of the 5G channels. Finally, the vehicular communications were started to be standardized with the D2D and through for the V2X, which is one the main topics of this work.

Vehicular communications are composed by a several ones, like the V2V, communications between two vehicles, the V2I, and vehicle communicate with an infrastructure like the infrastructure from a highway, the VIP, how the vehicle communicates with a pedestrian, like an person walk on the street and the more important the V2X, the communication between an vehicle to everything. Also, the evolution from the CV2X, starting with the release 11 as well the first type of communication between devices, the D2D going through the of spoken NR V2X in release 16. Besides the evolution to the NR V2X, it physical layer, which on more is on focus of this work, was analysed as well, it numerology and it specifications and the overall flow of waveform generation for sidelink. How the resources are distributed in time and as well in frequency domain, allocated and the definition of the 5G physical channels, like the PSSCH and consequently reference signals. The MIB, what are its main characteristics and how its message is composed and transmitted. Further the objective is defining the parameters of it message and how it is transmitted. Finally, the transport block, its characteristics how to obtain the size of it, first knowing the type of codification, for example QPSK, 16QAM, between others, that it is in the SCI. Finally, the discussion about the main differences between the LTE-V2X and the NR-V2X.

After all the studies that was required for this work, was developed an effective PSCCH searching algorithm for 5G-NR V2X sidelink communications, based on pre-existing algorithms. In the proposed approach, firstly was computed all the correlations between the received signal and the PSCCH DMRS, and the remaining conventional processing to decode the PSCCH is only performed over the subchannels with higher correlation The results showed that the proposed algorithm achieves the same performance in terms of SCI BLER and throughput, but with a much shorter runtime. Furthermore, the average number of attempts to decode the PSCCH always tends to 1 for high SNR, regard-less of bandwidth. Therefore, the proposed PSCCH searching algorithm could be an interesting approach for real-time systems, even for very high bandwidths, which are expected in 5G-NR communications.

Concluding this work, all the objectives for this dissertation was completely fulfilled, with the development of a new algorithm in search and decoding of the PSCCH, based in pre-existing ones, which was the main goal of this work.

5.2 – Future work

The proposed search/decoding PSCCH was evaluated in a simulation platform. However, it would be of practical interest to validate the algorithm in real-time, in other words in more realistic scenarios with the support of the company Allbesmart.

Moreover, this proposed algorithm is still limited mainly by the processing time from the correlation's calculations. The future work could be optimizing the correlation's calculations in order to minimize the referred time above, as well minimizing the overall processing time for this proposed algorithm.

The techniques and the work developed could also be a next step for other concepts like smart houses and smart cities. Vehicular communications are the head start for the possibilities that the 5G of mobile communications could bring for the future, in a more autonomous and intelligent city, the safety, an improved traffic manager.

References

[1] Ericsson, “Gsm System Survey Student Text,” *ReVision*, pp. 1–410, 1999.

[2] H. Mehta, D. Patel, B. Joshi, and H. Modi, “0G to 5G Mobile Technology: A Survey,” vol. 1, no. 6, pp. 56–60, 2014.

[3] M. Miri, “Hybrid Equalizer for millimeter wave GFDM Systems,” Tese de Dissertação em Engenharia Eletrónica e Telecomunicações, Universidade de Aveiro, 2020.

[4] M. R. Bhalla and A. V. Bhalla, “Generations of Mobile Wireless Technology: A Survey,” *Int. J. Comput. Appl.*, vol. 5, no. 4, pp. 26–32, 2010.

[5] M. A. M. Albreem, “5G wireless communication systems: Vision and challenges,” *I4CT 2015 - 2015 2nd Int. Conf. Comput. Commun. Control Technol. Art Proceeding*, no. I4ct, pp. 493–497, 2015.

[6] S. A. and A. Muhammad, “The Principle of OFDM and Use in 4g Radio Cellular Systems,” *Int. J. Comput. Appl.*, vol. 182, no. 27, pp. 46–49, 2018.

[7] M. Lopa and J. Vora, “Evolution of mobile generation technology: 1G to 5G and review of upcoming wireless technology 5G,” *Int. J. Mod. trends Eng. Res.*, vol. 2, no. 10, pp. 281–290, 2015.

[8] M. Harounabadi, D. M. Soleymani, S. Bhadauria, M. Leyh, and E. Roth-Mandutz, “V2X in 3GPP Standardization: NR Sidelink in Release-16 and beyond,” *IEEE Commun. Stand. Mag.*, vol. 5, no. 1, pp. 12–21, 2021.

[9] “K. Ganesan, J. Lohr, P. B. Mallick, A. Kunz and R. Kuchibhotla, ‘NR Sidelink Design Overview for Advanced V2X Service,’ in IEEE Internet of Things Magazine, vol. 3, no. 1, pp. 26-30, March 2020, doi: 10.1109/IOTM.0001.1900071.”

[10] K. Ganesan, P. B. Mallick, J. Lohr, D. Karampatsis, and A. Kunz, “5G V2X Architecture and Radio Aspects,” *2019 IEEE Conf. Stand. Commun. Networking, CSCN 2019*, 2019.

[11] T. Soni, A. R. Ali, K. Ganesan, and M. Schellmann, “Adaptive numerology - A solution to address the demanding QoS in 5G-V2X,” *IEEE Wirel. Commun. Netw. Conf. WCNC*, vol. 2018-April, pp. 1–6, 2018.

[12] A. Alalewi, I. Dayoub, and S. Cherkaoui, “On 5G-V2X Use Cases and Enabling Technologies: A Comprehensive Survey,” *IEEE Access*, vol. 9, pp. 107710–107737, 2021.

[13] S. Lien *et al.*, "3GPP NR Sidelink Transmissions Toward 5G V2X," *IEEE Access*, vol. 8, pp. 35368–35382, 2020.

[14] R. Shrestha, S. Y. Nam, R. Bajracharya, and S. Kim, "Evolution of v2x communication and integration of blockchain for security enhancements," *Electron.*, vol. 9, no. 9, pp. 1–33, 2020.

[15] T. T. T. Le and S. Moh, "Comprehensive Survey of Radio Resource Allocation Schemes for 5G V2X Communications," *IEEE Access*, vol. 9, pp. 123117–123133, 2021.

[16] "3GPP, 'TS 38.101-1: User Equipment (UE) radio transmission and reception, Part 1, Range 1 Standalone', Tech. Spec., Dec. 2020, v17.0.0."

[17] A. Bazzi, A. O. Berthet, C. Campolo, B. M. Masini, A. Molinaro, and A. Zanella, "On the Design of Sidelink for Cellular V2X: A Literature Review and Outlook for Future," *IEEE Access*, vol. 9, pp. 97953–97980, 2021.

[18] R. Molina-masegosa and J. Gozalvez, "LTE-V for Sidelink 5G V2X Vehicular Communications," no. December, 2017.

[19] B. Bangerter, S. Talwar, R. Arefi, and K. Stewart, "Networks and devices for the 5G era," *IEEE Commun. Mag.*, vol. 52, no. 2, pp. 90–96, 2014.

[20] J. C. Gallagher, "Technologies : Issues for Congress," 2019, [Online]. Available: https://www.everycrsreport.com/reports/R45485.html#_Toc966844.

[21] S. A. Busari, K. M. S. Huq, S. Mumtaz, L. Dai, and J. Rodriguez, "Millimeter-Wave Massive MIMO Communication for Future Wireless Systems: A Survey," *IEEE Commun. Surv. Tutorials*, vol. 20, no. 2, pp. 836–869, 2018.

[22] F. Rusek *et al.*, "Scaling up MIMO : Opportunities and challenges with very large arrays," *IEEE Signal Process. Mag.*, vol. 30, no. 1, pp. 40–60, 2013.

[23] M. Mimo and U. Gan, "Realizing 5G Sub-6-GHz Massive MIMO Using GaN," *microwaves &RF*, pp. 4–8, 2019.

[24] A. Shaikh and M. J. Kaur, "Comprehensive Survey of Massive MIMO for 5G Communications," *2019 Adv. Sci. Eng. Technol. Int. Conf. ASET 2019*, pp. 1–5, 2019.

[25] Z. Pi and F. Khan, "An introduction to millimeter-wave mobile broadband systems," *IEEE Commun. Mag.*, vol. 49, no. 6, pp. 101–107, 2011.

[26] C. R. Anderson and T. S. Rappaport, "In-building wideband partition loss measurements at 2.5 and 60 GHz," *IEEE Trans. Wirel. Commun.*, vol. 3, no. 3, pp. 922–928, 2004.

[27] J. M. Durante, "BUILDING PENETRATION LOSS AT 900 MHz.," no. May, 1973.

[28] A. V. Alejos, M. G. Sánchez, and I. Cuiñas, "Measurement and Analysis of Propagation Mechanisms at 40 GHz : Viability of Site Shielding Forced by Obstacles," vol. 57, no. 6, pp. 3369–3380, 2008.

[29] M. De Ree, G. Mantas, A. Radwan, S. Mumtaz, J. Rodriguez, and I. E. Otung, "Key Management for beyond 5G Mobile Small Cells: A Survey," *IEEE Access*, vol. 7, pp. 59200–59236, 2019.

[30] J. Paulo, L. Silva, S. Wanberg, R. S. Silva, and C. B. Both, "Minicurso : Entendendo o núcleo 5G na prática através de uma implementação de código aberto," no. October, pp. 22–25, 2020.

[31] T. Specification, "TS 138 323 - V16.2.0 - 5G; NR; Packet Data Convergence Protocol (PDCP) specification (3GPP TS 38.323 version 16.2.0 Release 16)," vol. 0, pp. 0–41, 2020.

[32] 3GPP TS 38.201, "5G; NR; Physical layer; General description (Release 15)," *3rd Gener. Partnersh. Proj. (3GPP), TS 138 201 - V15.0.0, V15.0.0*, vol. 0, pp. 0–13, 2018.

[33] T. Specification, "TS 138 215 - V16.2.0 - 5G; NR; Physical layer measurements (3GPP TS 38.215 version 16.2.0 Release 16)," vol. 0, 2020.

[34] TSGR, "TS 138 322 - V15.3.0 - 5G; NR; Radio Link Control (RLC) protocol specification (3GPP TS 38.322 version 15.3.0 Release 15)," vol. 0, pp. 0–35, 2018.

[35] T. Specification, "TS 137 324 - V16.2.0 - (3GPP TS 37.324 version 16.2.0 Release 16)," vol. 0, pp. 0–18, 2020.

[36] C. Johnson, "5G New Radio," *5G New Radio*, p. 590, 2019.

[37] A. Ghosh, A. Maeder, M. Baker, and D. Chandramouli, "5G Evolution: A View on 5G Cellular Technology beyond 3GPP Release 15," *IEEE Access*, vol. 7, no. March, pp. 127639–127651, 2019.

[38] J. Guerreiro and M. Marques da Silva, "O Contributo das Comunicações 5G para a 4ª Revolução Industrial."

[39] ETSI, "5G NR Physical channels and modulation (3GPP TS 38.211 version 15.2.0 Release 15)," *Ts 138 211 - V15.2.0*, vol. 2, pp. 1–98, 2018.

[40] A. A. Zaidi, R. Baldemair, H. Tullberg, H. Björkegren, L. Sundström, and J. Medbo, "Waveform and Numerolog y to Support 5G Services and Requirements," pp. 1–9.

[41] T. Specification, "TS 138 214 - V16.2.0 - 5G; NR; Physical layer procedures for data (3GPP TS 38.214 version 16.2.0 Release 16)," vol. 0, 2020.

[42] M. H. C. Garcia *et al.*, "A Tutorial on 5G NR V2X Communications," *IEEE Commun. Surv.*

Tutorials, vol. 23, no. 3, pp. 1972–2026, 2021.

[43] T. Specification, “TS 138 331 - V16.1.0 - 5G; NR; Radio Resource Control (RRC); Protocol specification (3GPP TS 38.331 version 16.1.0 Release 16),” vol. 0, 2020.

[44] W. Anwar, N. Franchi, and G. Fettweis, “Physical layer evaluation of V2X communications technologies: 5G NR-V2X, LTE-V2X, IEEE 802.11bd, and IEEE 802.11p,” *IEEE Veh. Technol. Conf.*, vol. 2019-Septe, pp. 1–7, 2019.

[45] Z. Ali, S. Lagen, L. Giupponi, and R. Rouil, “3GPP NR V2X Mode 2: Overview, Models and System-level Evaluation,” *IEEE Access*, vol. 9, p. 1, 2021.

[46] S. Kang and S. Choi, “A novel procedure of enhancing the throughput of a mode-2 sidelink based on partial sensing,” *Sensors*, vol. 21, no. 18, 2021.

[47] L. Cao and H. Yin, “Resource Allocation for Vehicle Platooning in 5G NR-V2X via Deep Reinforcement Learning,” *2021 IEEE Int. Black Sea Conf. Commun. Networking, BlackSeaCom 2021*, pp. 1–7, 2021.

[48] S. Hegde, O. Blume, R. Shrivastava, and H. Bakker, “Enhanced resource scheduling for platooning in 5G V2X systems,” *IEEE 5G World Forum, 5GWF 2019 - Conf. Proc.*, pp. 108–113, 2019.

[49] S. Lee, J. Kim, J. Park, and S. Cho, “Grant-free resource allocation for NOMA V2X uplink systems using a genetic algorithm approach,” *Electron.*, vol. 9, no. 7, pp. 1–15, 2020.

[50] “Zhao et al., ‘Cluster-Based Resource Selection Scheme for 5G V2X,’ 2019 IEEE 89th Vehicular Technology Conference (VTC2019-Spring), 2019, pp. 1-5.”

[51] F. Abbas, G. Liu, Z. Khan, K. Zheng, and P. Fan, “Clustering based resource management scheme for latency and sum rate optimization in V2X networks,” *IEEE Veh. Technol. Conf.*, vol. 2019-April, no. Cm, pp. 1–6, 2019.

[52] X. Song, K. Wang, L. Lei, L. Zhao, Y. Li, and J. Wang, “Interference Minimization Resource Allocation for V2X Communication Underlaying 5G Cellular Networks,” *Wirel. Commun. Mob. Comput.*, vol. 2020, 2020.

[53] F. Abbas, G. Liu, P. Fan, Z. Khan, and M. S. Bute, “A Vehicle Density based Two-Stage Resource Management Scheme for 5G-V2X Networks,” *IEEE Veh. Technol. Conf.*, vol. 2020-May, pp. 1–5, 2020.

[54] R. Magueta, J. Domingues, A. Silva, and P. Marques, “Effective PSCCH searching for 5G-NR V2X sidelink communications,” *Electron.*, vol. 10, no. 22, pp. 1–15, 2021.

[55] 3GPP, “Physical channels and modulation (3GPP TS 38.211 version 15.3.0 Release 15),” vol. 0, 2020.

[56] 3GPP, “TS 138 213 - V15.8.0 - 5G; NR; Physical layer procedures for control (3GPP TS 38.213 version 15.8.0 Release 15),” vol. 0, pp. 0–94, 2020.

[57] R. Magueta, D. Castanheira, P. Pedrosa, and R. Dinis, “Wideband Millimeter Wave Massive MIMO Systems,” *Sensors 2020, 20, 575*, 2020.